The Journal of Neuroscience, September 15, 1996, *16*(18):5629–5643

Rapid, Active Hair Bundle Movements in Hair Cells from the Bullfrog's Sacculus

Michael E. Benser, Robert E. Marquis, and A. J. Hudspeth

Howard Hughes Medical Institute and Laboratory of Sensory Neuroscience, The Rockefeller University, New York, New York 10021

Hair bundles, the mechanically sensitive organelles of hair cells in the auditory and vestibular systems, are elastic structures that are deflected by sound or acceleration. To examine rapid mechanical events associated with mechanoelectrical transduction, we stimulated individual hair bundles with flexible glass fibers and measured their responses with a temporal resolution of 400 μsec. When a hair bundle from the bullfrog's sacculus was abruptly deflected in the positive direction, the bundle's motion in the direction of stimulation was interrupted within the initial few milliseconds by an active movement, or twitch. This response was biphasic, with an initial component in the direction of the stimulus and a second component in the opposite direction. The amplitude and duration of the twitch depended on the bundle's initial position and the size and rise time of the stimulus; the twitch was largest over the range of bundle deflections in which transduction was most sensitive. Under displacement clamp conditions, in which a hair bundle's position was changed and then held constant with negative feedback, the twitch manifested itself as a biphasic force exerted by the bundle. Some hair bundles produced twitches in response to negatively directed stimuli, exhibited stimulus-evoked damped oscillations, or twitched spontaneously. The hair bundle's ability to perform work against an external load and to oscillate in response to stimulation indicates that the bundle could supply feedback for mechanical amplification in vertebrate auditory organs.

Key words: auditory system; frog; hair bundle; hair cell; ion channel; mechanics; mechanoelectrical transduction; myosin; vestibular system

The detection of sound and acceleration rests on mechanoelectrical transduction by hair cells, the receptors of the vertebrate auditory and vestibular systems. The hair cell's mechanically sensitive organelle is the hair bundle, which comprises tens to hundreds of actin-filled rods, the stereocilia, and a single true cilium, the kinocilium, standing in ranks of progressively increasing height. A hair cell is stimulated when this elastic bundle is deflected toward its tall edge (for review, see Hudspeth, 1989). With the hair bundle in its resting position, ~15% of a cell's 100 or so transduction channels are open. Movement of the bundle in the positive direction, toward its tall edge, opens additional channels; negative stimulation, by contrast, closes a portion of the channels open at rest. The small latency of mechanoelectrical transduction indicates that the channels are directly gated by mechanical force (Corey and Hudspeth, 1979); the gating springs that control channel opening (Corey and Hudspeth, 1983) are probably tip links, filaments connecting adjacent stereocilia near their tips (Pickles et al., 1984). Prolonged bundle deflection elicits adaptation, a process in which the transduction channels' open probability returns toward its resting level (Eatock et al., 1987).

The mechanical properties of hair bundles have been extensively characterized by measuring bundle motion in response to forces applied by flexible glass fibers of calibrated stiffness. In addition to their passive stiffnesses (for review, see Howard et al., 1988), bundles display mechanical responses associated with channel gating (Howard and Hudspeth, 1988) and adaptation (Howard and Hudspeth, 1987a). Moreover, a limited number of observations indicate that hair bundles are capable of other motile responses. Spontaneous hair bundle movements include components too large to stem from Brownian motion; in addition, abrupt displacements can evoke bundle oscillations (Crawford and Fettiplace, 1985; Howard and Hudspeth, 1987a; Denk and Webb, 1992). Finally, rapid deflection can trigger twitches of a hair bundle (Howard and Hudspeth, 1987a,b, 1988; Jaramillo et al., 1990), the subject of the present study (Marquis et al., 1995).

There are three reasons for an interest in the fast motile activity of hair bundles. First, because bundle deflection directly opens and closes transduction channels, mechanical measurements may shed light on rapid events in the gating process. Second, because adaptation probably involves myosin-based adjustment of the tension in gating springs (for review, see Hudspeth and Gillespie, 1994), such measurements may detect the stepping activity of individual or clustered myosin molecules. Third, mechanical measurements may identify the active process responsible for signal amplification and otoacoustical emissions in the auditory system (for review, see Probst, 1990; Dallos, 1992). In the mammalian cochlea, the contractile activity of outer hair cells is thought to account for amplification. Contractile outer hair cells are confined

Received April 24, 1996; revised June 27, 1996; accepted July 2, 1996.

M.E.B. and R.E.M. contributed equally to this research. Begun at University of Texas Southwestern Medical Center, this work was supported by National Institutes of Health Grant DC00317. A.J.H. is an Investigator of Howard Hughes Medical Institute. We thank Dr. J. Howard for advice about mechanical measurements and for access to his previous experimental results, Dr. L. F. A. Jaramillo for suggestions about displacement clamp recording, Dr. K. Behbehani for assistance with stabilization of the displacement clamp system, and Dr. J. M. Phelps for computer programming. Drs. L. Avery, S. T. Brady, D. W. Hilgemann, and J. Howard and members of our research group kindly provided comments on this manuscript; the two reviewers' five-page critique also focused our thoughts.

Correspondence should be addressed to Dr. A. J. Hudspeth, Howard Hughes Medical Institute and Laboratory of Sensory Neuroscience, Box 314, The Rockefeller University, 1230 York Avenue, New York, NY 10021-6399.

Dr. Benser's current address: Guidant Corporation, 4100 Hamline Avenue North, St. Paul, MN 55112-5798.

to mammals, however, whereas amplification is ubiquitous in vertebrate auditory systems. Active motility by hair bundles, powered by channel gating (Howard and Hudspeth, 1988; Jaramillo et al., 1990) or by myosin stepping (for review, see Hudspeth and Gillespie, 1994), could provide an additional mechanism for augmenting mechanical signals in the internal ear.

MATERIALS AND METHODS

Experimental preparation. Experiments were conducted at room temperature (21–26°C) on individual hair cells in the macular epithelium from the bullfrog, *Rana catesbeiana*. Internal ears were removed from doubly pithed animals and transferred to an oxygenated saline solution containing (in mM): 110 Na^+, 2 K^+, 4 Ca^{2+}, 118 Cl^-, 3 D-glucose, and 5 HEPES. The solution's osmotic strength was ~230 mmol · kg^{-1}; its pH was adjusted to 7.25.

After isolation of the sacculus and removal of its otoconia, the compact otolithic membrane was enzymatically separated from the underlying hair bundles by treatment for 20–60 min with 20–50 mg · l^{-1} subtilopeptidase A (synonymous with subtilisin Carlsberg and protease type VIII; Sigma, St. Louis, MO) in saline solution. After the otolithic membrane had been gently peeled away with an eyelash, the epithelial preparation was secured with metal clips to the coverslip bottom of a 500 μl experimental chamber. To prolong its activity, the preparation was periodically bathed in fresh, oxygenated saline solution. When indicated, we substituted a gentamycin saline solution supplemented with 100 μM gentamycin sulfate (Sigma). A few control experiments were conducted containing (in mM): 110 Na^+, 2 K^+, 0.25 Ca^{2+}, 111 Cl^-, 3 D-glucose, and 5 HEPES.

Preparations were observed with a mechanically stabilized upright microscope (UEM, Zeiss, Jena, Germany) equipped with differential interference contrast optics. Illuminated by a 100 W mercury arc lamp (HBO 100, Zeiss), sensory epithelia were examined through a 40× water immersion objective lens of numerical aperture 0.75, a 1.6× accessory lens, and 10× oculars. To minimize mechanical noise, the microscope was mounted on an internally damped, air-suspended table (GS-34-FR, Newport Bio-Instruments, Fountain Valley, CA) within an acoustically isolated room constructed on a concrete pad.

Membrane potential measurement. In most experiments, each hair cell's membrane potential was recorded during mechanical stimulation. Microelectrodes were fabricated with an electrode puller (P-80/PC, Sutter Instrument, Novato, CA) such that their resistances were 100–300 MΩ when filled with an internal solution of 3 M KCl buffered to a pH of 8.5 with 10 mM glycylglycine (Thomas, 1978). To facilitate cellular penetration in the restricted space set by the 1.6 mm working distance of the objective lens, electrodes were bent through an angle of ~60° about 0.5 mm from their tips (Hudspeth and Corey, 1978). With a Huxley-type micromanipulator (Frederick Haer, Brunswick, ME), each electrode was inserted into an apical cellular surface adjacent to the hair bundle's short edge, the side opposite the stimulus fiber's usual attachment. Membrane potential recordings were referenced to the bath's potential with a direct-coupled amplifier operated in bridge mode (Axoclamp-2A, Axon Instruments, Foster City, CA). The amplifier's capacitance compensation was adjusted for a passband of ~0-1 kHz.

Mechanical stimulation. Hair bundles were displaced with flexible stimulus fibers fabricated from borosilicate glass rods 1.2 mm in diameter (Kimble KG-33, Garner Glass, Claremont, CA). Each fiber was first reduced with an electrode puller, then pulled still finer in a direction perpendicular to its shank (Howard and Hudspeth, 1988). To facilitate measurement of the fiber tip's position, the fiber's optical contrast was increased by coating it with an ~100 nm layer of gold palladium (Hummer VI, Anatech, Alexandria, VA). A fiber was lastly trimmed with fine iris scissors (Moria 9600, Fine Science Tools, Foster City, CA) until its stiffness and damping constant were 200–1200 μN · m^{-1} and 50–400 nN · sec · m^{-1}, respectively, as determined by analysis of the power spectrum of the tip's Brownian motion in water (Howard and Hudspeth, 1988; Denk et al., 1989). The tip of a finished fiber measured 400–500 nm in diameter.

A fiber was horizontally mounted at its base in a holder attached to a stack-type piezoelectrical actuator (P835.10, Physik Instrumente, Waldbronn, Germany), which was in turn secured to a Huxley-type micromanipulator. Driven by a matched power supply (P-870, Physik Instrumente), the actuator could produce calibrated displacements of at least ±1 μm with a bandwidth exceeding 5 kHz. Using the displacement monitor described below, we measured the movements of an unimpeded fiber in response to the application of a range of voltage steps to the actuator. Knowing the relation between actuator output and applied voltage, we could infer the position of the fiber's base during experiments from the voltage.

Most experiments were conducted on large hair cells near the abneural edge of the saccular macula; a few experiments confirmed that small hair bundles can also produce twitches. Except when specifically noted, the microscope's stage was rotated such that each hair bundle was displaced along its axis of morphological symmetry, and therefore greatest mechanical sensitivity (Shotwell et al., 1981). Hair bundle motion was usually elicited by affixing the tip of a stimulus fiber to the free surface of the kinociliary bulb (Fig. 1*A*). In a few experiments, the fiber's tip was instead applied to the sides of the hair bundle's shortest stereocilia, the bundle surface opposite the kinocilium.

Experiments in which square pulses of displacement were delivered to a fiber's base were termed "base movement" experiments, whereas those in which the fiber's tip was commanded to produce displacement pulses under negative feedback conditions were denoted "displacement clamp" experiments. Computer generated as square-pulse templates, stimuli were usually delivered as trains of successive templates that varied in the value of one parameter. Unless otherwise indicated, the interval between presentations of successive templates within a stimulus train was 400 msec.

Displacement monitor. Movements of a stimulus fiber were measured with a displacement monitor mounted atop the microscope's vertical camera port. With a 12.5× ocular in the trinocular tube, the height of the monitor was adjusted to provide a magnification of 1000× there. The displacement monitor was attached to the camera port by a closed-loop micrometer actuator (850B-05, Newport, Irvine, CA) powered by a matched-motion controller (PMC100, Newport), which could horizontally translate the displacement monitor over a 13 mm range with a precision of 0.1 μm. Because of the optical magnification, the system could thus accomplish a movement equivalent at the level of the specimen to 13 μm with a precision of 0.1 nm.

Within the displacement monitor, the image of a fiber's tip was projected onto a photodiode pair (UV-140-2, EG & G Electro-Optics, Salem, MA). A pair of current-to-voltage converters and a differential amplifier produced an output voltage proportional to the difference in light received by the two photodiodes (Fig. 1*A*). When centered over the image of a stimulus fiber's tip, the monitor registered 0 V; movement of the tip caused the output to change linearly over a range approximately equal to the fiber's radius.

The gain of the displacement monitor, or the ratio of output voltage to fiber tip displacement, was determined in base movement experiments by computer activation of a calibration piezoelectrical actuator with a dedicated amplifier (PZL-030 and PZ-150 M, Burleigh Instruments, Fishers, NY), which served to displace the monitor's photodiode pair (Art et al., 1986; Howard and Hudspeth, 1987a). Immediately before each stimulus fiber command, the computer issued a template-based command for the calibration actuator to move the photodiode pair by a known amount, usually 20 μm. Through this calibrated motion pulse and knowledge of the optical magnification at the level of the displacement monitor, the output voltage was converted to an equivalent displacement value for subsequent data analysis.

Displacement clamp force measurement. Negative feedback circuitry was used to measure the force exerted by a hair bundle when it was displaced and subsequently held at a new position. In such a displacement clamp experiment, the command signal was first compared with the displacement monitor output representing the fiber tip's position, then the difference between these signals was amplified and delivered to the stimulus fiber actuator.

In earlier work, a phase lag, in the form of a parallel capacitor, was introduced in the feedforward circuit to maintain stability at high loop gains (Jaramillo and Hudspeth, 1993). This approach so limited the system's bandwidth that the bundle's rise time to a step command could not be decreased to <3 msec, a rise time usually too long to elicit the phenomena studied here. To obtain the bandwidth necessary for clamping more rapid motions, a single-pole phase-lead controller (Ogata, 1970) was added in series with the capacitor. After this modification (Benser, 1995), the system's bandwidth was dominated by the mechanical resonance of the stimulus-fiber actuation system. By minimization of a fiber's shank length, typically to <20 mm, we raised this resonant frequency above 1 kHz; we could thus make displacement clamp measurements with a temporal resolution comparable to that obtained in base movement experiments.

The elastic force exerted by the stimulus fiber to maintain a hair

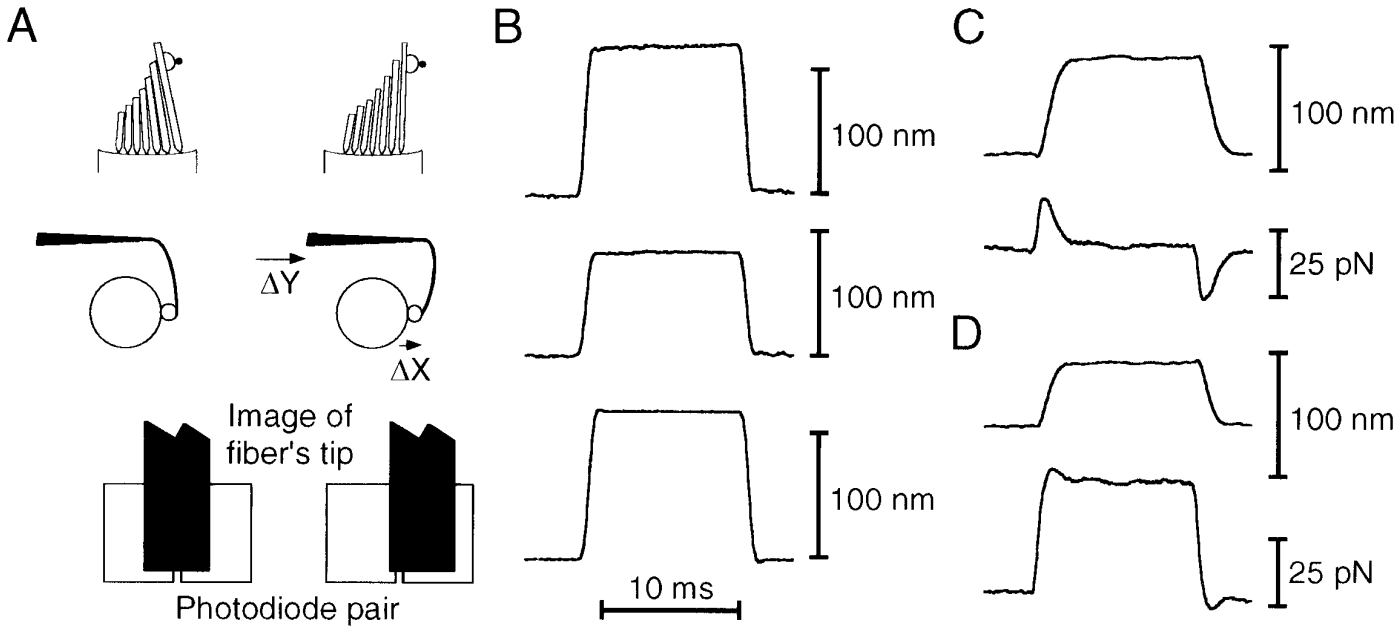

Figure 1. The experimental system and control experiments. *A*, In preparation for stimulation, the stimulus fiber's tip was brought into contact with the bundle at its kinociliary bulb, and the displacement monitor was centered over the fiber's tip. After application of a displacement to the fiber's base, the bundle's resultant movement was measured by the displacement monitor. The displacement monitor reported a voltage that was proportional to the difference in light received by its two photocells. *B*, In a base movement experiment, the base of a stimulus fiber of stiffness 1190 $\mu N \cdot m^{-1}$ was abruptly displaced (*bottom trace*). When the fiber's tip was unengaged, it followed the displacement pulse with high fidelity (*top trace*). When the same fiber's tip was attached to a flexible glass filament of stiffness 511 $\mu N \cdot m^{-1}$, the tip's movement (*middle trace*) was diminished as a result of the stimulus fiber's flexion. *C*, Under displacement clamp conditions, the tip displacement of an unloaded stimulus fiber of stiffness 595 $\mu N \cdot m^{-1}$ (*top trace*) essentially reached its final value within 2 msec. The force measured by the clamp system (*bottom trace*) reflected the viscous drag on the fiber, whose drag coefficient was 198 $nN \cdot sec \cdot m^{-1}$. *D*, When the same fiber was attached to a flexible glass filament of stiffness 820 $\mu N \cdot m^{-1}$, the tip motion (*top trace*) was equally fast. The clamp force (*bottom trace*) showed both a steady-state component attributable to the elastic load and transients arising from viscous drag. The data for panels *B*, *C*, and *D* were filtered at 10 kHz and sampled at 25 kHz; each trace is the average of 10 responses.

bundle's deflection was computed from the product of the fiber's flexion and stiffness. The bundle's restoring force was equal to the fiber's elastic force less any hydrodynamic drag introduced by movement of the fiber and bundle. Each fiber's damping constant was estimated from its Brownian motion; the bundle's damping constant was assumed to be 200 $nN \cdot sec \cdot m^{-1}$ (Howard and Hudspeth, 1988). The acceleration of the hair bundle and the stimulus fiber tip never exceeded 400 $mm \cdot sec^{-2}$, so the associated inertial forces were <1 pN. Because the force produced by a hair bundle was 50 pN in most experiments, these inertial forces were neglected.

The gain of the displacement monitor in base movement experiments was determined by calibrated displacement of the photodiode pair immediately before each stimulus. Because of feedback movement of the stimulus fiber during displacement clamp experiments, the displacement monitor's gain was determined within 1 min before or after each set of recordings. While the fiber was held at a constant position, the changes in output voltage resulting from the application of calibrated step motions were measured with the displacement monitor. The slope of the least-squares linear fit to this relation, scaled by the optical magnification, yielded the displacement monitor's gain. During a displacement clamp experiment, the system's response to the motion of the displacement monitor before each stimulus provided a measure of the efficacy of clamping.

Data collection and analysis. A computer (Quadra 800, Apple Computer, Cupertino, CA) controlled the stimulus fiber and photodiode calibration actuators through an interface (NB-AO-6, National Instruments, Austin, TX) equipped with 12-bit digital-to-analog converters. Except when otherwise indicated, computer outputs to the photodiode calibration and stimulus fiber actuators were filtered with eight-pole Bessel filters (852, Wavetek, San Diego, CA) at half-power frequencies of 20 Hz and 0.5–1.5 kHz, respectively. Unless otherwise noted, the displacement monitor and membrane potential outputs were filtered at 1.0 kHz, sampled with 12-bit analog-to-digital converters, and communicated to the computer at 2.5 kHz through an interface and direct memory access module (NB-A2000 and NB-DMA2800, National Instruments).

Software was written in LabVIEW (versions 3.0.1 and 3.1, National Instruments). Data analysis was performed on computers (Quadra 700, 800, and 840AV, Apple Computer) using LabVIEW and Excel (version 5.0, Microsoft, Redmond, WA). Figures were prepared for publication with Canvas (version 3.5, Deneba Software, Miami, FL).

Theoretical performance of the stimulation system. Measurements of a hair bundle's steady-state properties rely on the linear elasticity of glass fibers and the application of Hooke's law (Okuno and Hiramoto, 1979). Because there is no literature concerning the use of such fibers in the measurement of transient bundle motions, it is necessary to define the limitations on measurements made with high temporal resolution. The use of a novel displacement clamp system additionally mandates analysis of its theoretical performance.

Suppose that, by displacement of a stimulus fiber's base through a distance Y, a hair bundle is abruptly deflected by an amount, X, that is a function of time. Let the stiffnesses of the fiber and bundle be K_{SF} and K_{HB}, respectively, and the drag coefficients for the fiber and bundle be ξ_{SF} and ξ_{HB}, respectively. In addition, make the simplifying assumptions that inertial terms may be neglected and that drag is concentrated at the fiber's tip and bundle's top, rather than distributed along both the fiber and the bundle. Finally, let F_A represent a time-dependent force produced within the hair bundle; a positive sign for this force corresponds to a force that pushes the stimulus fiber in the positive direction.

At any time, the force exerted by the fiber against the bundle and that produced by the bundle on the fiber are equal and opposite, so the total force provided by the fiber, F_{SF}, is:

$$F_{SF} = K_{SF}(Y - X) = (\xi_{SF} + \xi_{HB})\frac{dX}{dt} + K_{HB}\,X - F_A. \qquad (1)$$

If a step displacement is applied at the fiber's base at the time $t = 0$, the bundle's motion is described by:

$$X = \left(\frac{K_{SF}}{K_{SF} + K_{HB}}\right) Y(1 - e^{-t/\tau}) + \left(\frac{1}{\xi_{SF} + \xi_{HB}}\right) e^{-t/\tau} \int F_A\, e^{T/\tau}\, dT, \qquad (2)$$

where τ is the time constant characterizing the hair bundle's relaxation and T is an integration variable.

The practical consequence of this relation can be seen by evaluating the system's response to a plausible active force generated by the hair bundle. Although any arbitrary force might be considered, including a very general one such as a delta function, it is simplest to calculate the response to a force step of constant magnitude F_S beginning with the externally imposed bundle deflection and persisting indefinitely thereafter. In this instance,

$$X = \left(\frac{1}{K_{SF} + K_{HB}}\right)(K_{SF}Y + F_s)(1 - e^{-t/\tau}). \quad (3)$$

Immediately after application of the stimulus, the bundle remains in its resting position. Much later, the bundle's displacement reaches a steady level determined by both the bundle's stiffness and the enduring force production. The two components rise exponentially toward their plateau levels at rates determined by the same time constant. The force exerted by the fiber is:

$$F_{SF} = \left(\frac{K_{SF}}{K_{SF} + K_{HB}}\right)[(K_{SF}\, e^{-t/\tau} + K_{HB})Y - F_s(1 - e^{-t/\tau})]. \quad (4)$$

The negative sign of the active-force term indicates that a positively directed force generated within the bundle reduces the force that the stimulus fiber must provide to effect a given positive bundle displacement.

Of critical importance in both relations are the time constant and the associated corner (cutoff) frequency, f_C, which are given by:

$$\tau = \left(\frac{\xi_{SF} + \xi_{HB}}{K_{SF} + K_{HB}}\right) \quad \text{and} \quad f_C = \frac{1}{2\pi\tau} = \frac{1}{2\pi}\left(\frac{K_{SF} + K_{HB}}{\xi_{SF} + \xi_{HB}}\right). \quad (5)$$

Our ability to measure the bundle's passive motion and our capacity to resolve active forces are both constrained in a similar way by the time constant. We wish to minimize the time constant so as to most precisely evaluate the bundle's properties, especially the time course and magnitude of the active force and their dependence on the extent and rate of bundle motion. The values of K_{HB} and ξ_{HB} are not subject to modification and are likely to be similar for a broad range of hair cells with bundles of similar dimensions. The temporal responsiveness of the measurement system can therefore be improved in only two ways: by decreasing the drag coefficient of the fiber, ξ_{SF}, or by increasing the fiber's stiffness, K_{SF}. The former route offers only limited hope, for decreasing the fiber's drag coefficient ceases to be of significance after that parameter's value becomes substantially less than the bundle's coefficient of 130–200 $nN \cdot sec \cdot m^{-1}$ (Howard and Hudspeth, 1988; Denk et al., 1989). Increasing the fiber's stiffness would appear to be a more promising strategy: if the fiber is appreciably more rigid than a hair bundle, whose dynamic stiffness in the frog's sacculus is $\sim$1000 $\mu N \cdot m^{-1}$ (Howard and Hudspeth, 1987a, 1988; Jaramillo and Hudspeth, 1993), then the time constant is inversely proportional to the fiber's stiffness.

Why is a very stiff fiber not desirable? Our capacity to measure a bundle's mechanical properties rests on our ability to measure a fiber's flexion. If the fiber becomes too stiff, its deflection is insignificant, and our ability to measure small displacements and forces vanishes. It is possible to estimate the stiffness of the most rigid fiber that would be useful. Brownian motion sets an absolute limit on the motion that we can measure with high temporal resolution; by the principle of equipartition of energy, the root mean square (RMS) thermal motion expected at the tip of a fiber attached to a hair bundle is:

$$X_{RMS} = \sqrt{\frac{kT}{K_{SF} + K_{HB}}}, \quad (6)$$

where k is the Boltzmann constant and T is the thermodynamical temperature. The minimal force that we can measure, $F_{RMS(MIN)}$, is determined by the smallest resolvable displacement:

$$F_{RMS(MIN)} = (K_{SF} + K_{HB})X_{RMS} = \sqrt{kT(K_{SF} + K_{HB})}. \quad (7)$$

This result demonstrates that increasing the fiber's stiffness improves temporal resolution, but unfortunately does so at the expense of displacement sensitivity. If we were to accept an RMS force sensitivity of, for example, 3 pN, the greatest permissible fiber stiffness would be $\sim$1200 $\mu N \cdot m^{-1}$. For a fiber and hair bundle of the stiffnesses and drag coefficients discussed throughout this paper, the associated time constant would be $\tau \approx 400$ μsec, and hence the corner frequency would be $f_C \approx 400$ Hz. Using conventional, base movement stimulation, there appears to be no means of escaping the limitation imposed by the time constant.

The displacement clamp configuration can potentially improve this situation. With this system, the output of the displacement monitor is compared with the displacement command signal, V_C, in a high-gain differential amplifier, the output of which serves as an error signal that is fed back to the stimulus fiber actuator. Let the amplifier's gain be G. Suppose, moreover, that the displacement monitor's output, V_D, is directly proportional to the displacement of the fiber's tip: $V_D = \alpha X$. Finally, assume that the actuator's displacement output, the fiber's base displacement Y, is directly proportional to the error signal, V_E: $Y = \beta V_E$. The equations that describe the displacement clamp system,

$$V_E = G(V_C - V_D) = G(V_C - \alpha X) = \frac{Y}{\beta} \quad \text{and} \quad F_{SF} = K_{SF}(Y - X), \quad (8)$$

may be combined to produce an expression for the total force exerted by the stimulus fiber under clamp conditions,

$$F_{SF} = K_{SF}[\beta G V_C - (\alpha\beta G + 1)X]. \quad (9)$$

If the displacement command is a step function, we obtain from this relation and Equation 1 the expected bundle motion:

$$X = \left[\frac{\beta G K_{SF}}{(\alpha\beta G + 1)K_{SF} + K_{HB}}\right]V_C(1 - e^{-t/\tau}) + \left(\frac{1}{\xi_{SF} + \xi_{HB}}\right)e^{-t/\tau}\int F_A e^{T/\tau}\, dT. \quad (10)$$

If the active force produced by a hair bundle is again a maintained step of amplitude F_S,

$$X = \left[\frac{1}{(\alpha\beta G + 1)K_{SF} + K_{HB}}\right](\beta G K_{SF} V_C + F_S)(1 - e^{-t/\tau}). \quad (11)$$

Note that the time constant and corner frequency for displacement clamp recording differ from those obtained for conventional stimulation; under displacement clamp conditions,

$$\tau = \left[\frac{\xi_{SF} + \xi_{HB}}{(\alpha\beta G + 1)K_{SF} + K_{HB}}\right] \text{ and } f_C = \frac{1}{2\pi}\left[\frac{(\alpha\beta G + 1)K_{SF} + K_{HB}}{\xi_{SF} + \xi_{HB}}\right]. \quad (12)$$

If the amplifier's gain is very great, we find that:

$$X \approx \frac{V_C}{\alpha}(1 - e^{-t/\tau}). \quad (13)$$

In this instance, the hair bundle follows the commanded step displacement with its relaxation rate set by the system's time constant, but undergoes no displacement due to the active force. With a high amplifier gain, the time constant and corresponding corner frequency approach the limiting values:

$$\tau \approx \left(\frac{\xi_{SF} + \xi_{HB}}{\alpha\beta G K_{SF}}\right) \quad \text{and} \quad f_C \approx \frac{1}{2\pi}\left(\frac{\alpha\beta G K_{SF}}{\xi_{SF} + \xi_{HB}}\right). \quad (14)$$

The gain of the clamp system is thus of critical importance, for increasing the gain decreases the time constant and raises the corner frequency. It is therefore potentially possible to obtain better temporal resolution under displacement clamp conditions than with conventional, base movement stimulation. According to this simplified analysis, there is no theoretical limit to the effect of increased gain. The practical limit to the system's temporal responsiveness is set by deviations of the actual apparatus from the theoretical ideal, for example, by noise in the displacement monitor and clamp amplifier. In addition, the occurrence of higher-order flexural modes in stimulus fibers (Gittes et al., 1993) slows a fiber's response and makes the time course of its relaxation more complex than that described by a single exponential relation.

With the bundle's position successfully controlled by the clamp system, we may inquire how the fiber's base moves; it is this signal that is useful in determining the force exerted by the clamp system to counter the

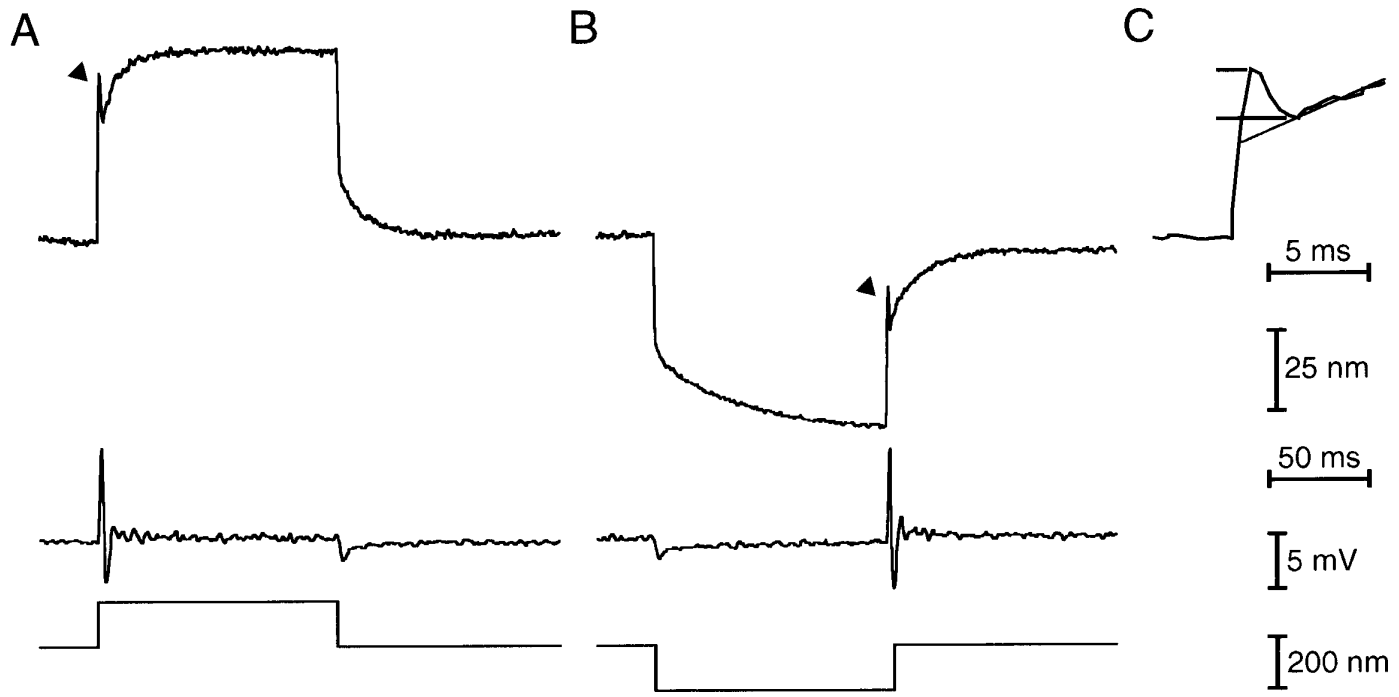

Figure 2. The hair bundle's evoked mechanical twitch. *A*, A hair bundle was stimulated by application of a 175 nm displacement pulse (*bottom trace*) at the base of a flexible fiber whose tip was coupled to the bundle's top. After displacement of the bundle toward its tall edge, a positive stimulus, the bundle's movement (*top trace*) in the direction of the applied force was briefly interrupted by a biphasic twitch (*arrowhead*). A spike of depolarizing receptor potential (*middle trace*) coincided with the twitch. *B*, When the same hair bundle was subjected to a negative displacement pulse of an identical magnitude, a twitch and transient depolarization occurred during the positively directed bundle motion at the end of the stimulus (*arrowhead*). *C*, A temporally expanded presentation of the bundle motion in *A* demonstrates the measurement of a twitch's size. The amplitude of a twitch was taken as the displacement between its peak and nadir, as shown by the *coarse horizontal lines*. Back-extrapolation of the subsequent bundle motion (*fine line*) yielded an alternative, larger estimate of a twitch's size. The *upper time calibration* applies only to *C*. All traces are averages of 10 records. The fiber's stiffness was 293 $\mu N \cdot m^{-1}$; the cell's resting potential was −63 mV.

passive and active forces produced by the bundle. Although the expressions for base displacement and fiber force are complicated, they assume simpler forms when the amplifier's gain is very high. In that instance,

$$Y \approx \beta G V_C e^{-t/\tau} - \left(\frac{F_S}{K_{SF}}\right)(1 - e^{-t/\tau}). \quad (15)$$

The force exerted by the stimulus fiber is then:

$$F_{SF} \approx \beta G K_{SF} V_C e^{-t/\tau} - F_S(1 - e^{-t/\tau}). \quad (16)$$

We should therefore measure a large but brief force transient associated with repositioning of the bundle, after which the active force's effect should be observed, filtered by the time constant associated with the clamp system.

Actual performance of the stimulation system. Before characterizing the rapid movements of hair bundles, we experimentally tested whether the stimulation system behaved in the theoretically predicted way. We also wished to ensure that the system was free of artifacts that might be confused with transient mechanical responses of hair bundles. It is known, for example, that rapid mechanical stimulation with a flexible fiber can produce "whiplash" or "back-flip" movements (Crawford and Fettiplace, 1985), in which the fiber's tip initially moves in the direction opposite the displacement imposed at the fiber's base. In addition, the high-frequency components of stimulus pulses can excite resonance in the actuator or fiber, leading to oscillation of the fiber's tip.

When the base of an unencumbered stimulus fiber was displaced by an amount typical of the experiments in this study, the fiber's tip faithfully followed the square displacement command (Fig. 1*B*). When the stimulus fiber was placed in contact with a glass filament of stiffness similar to that of a hair bundle, the loaded stimulus fiber was again well behaved throughout a rapid displacement. As long as a load, when present, was applied at a fiber's tip, and as long as the tip's image was properly centered on the photodiode pair, whiplash motions and other artifacts were never observed.

We additionally confirmed that the displacement clamp system operated as expected. With the system appropriately adjusted, a fiber's tip typically achieved 95% of the commanded displacement despite the load imposed by an attached hair bundle (Fig. 10). When commanded to move under displacement clamp conditions, even a relatively compliant stimulus fiber reached its final position within 2 msec (Fig. 1*C*). This performance was not significantly degraded by attaching the fiber to a glass filament of stiffness similar to that of a hair bundle (Fig. 1*D*).

RESULTS

The evoked hair bundle twitch

After deflection with a flexible stimulus fiber, a hair bundle displayed a complex pattern of motion (Fig. 2). At the onset of the displacement, the bundle underwent a rapid excursion in the direction of the stimulus. This fast response, as well as the oppositely directed fast movement at the end of the stimulus pulse, reflected the bundle's passive elastic reactance. During a protracted stimulus, the hair bundle also displayed a slow relaxation in the direction of the stimulation, typically with a time constant near 25 msec, indicative of adaptation (Howard and Hudspeth, 1987a). This mechanical correlate of adaptation also occurred in the opposite direction at the cessation of the displacement pulse.

Within a few milliseconds of the onset of a positive stimulus, a bundle's response was punctuated by a mechanical transient: the transition between the bundle's immediate displacement and the onset of adaptation was marked by a brief, biphasic twitch (Fig. 2*A*). A similar twitch response occurred at the termination of a negative bundle displacement (Fig. 2*B*). In each instance, the initial component of the twitch, movement in

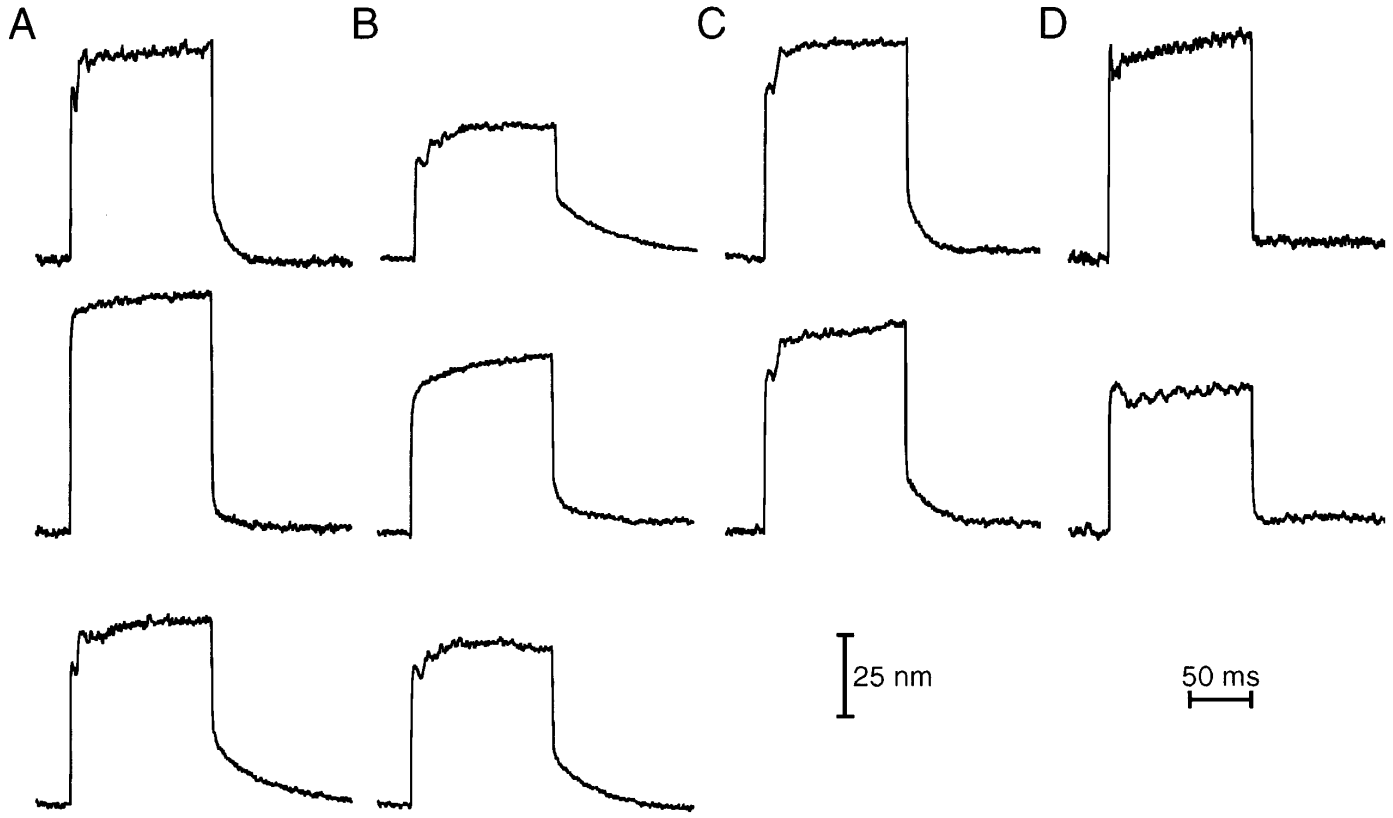

Figure 3. Control experiments. *A*, A twitch occurred after stimulation of a hair bundle in the positive direction (*top trace*). When the same bundle was stimulated in an orthogonal direction, however, the twitch was absent (*middle trace*). The response returned when the direction of stimulation was restored to the bundle's plane of symmetry (*bottom trace*). The slow bundle relaxation in the middle panel likely reflected a stimulus that was not perfectly perpendicular to the bundle's axis of responsiveness. *B*, A twitch occurred in the saline solution used for most experiments (*top trace*). Substitution of saline solution containing 100 μM gentamicin suppressed the twitch (*middle trace*), which returned after restoration of the original solution (*bottom trace*). After exposure to aminoglycoside drugs, both evoked and spontaneous twitching were potentiated for several minutes (J. Howard, personal communication). *C*, An intact hair bundle produced a twitch (*top trace*). This response was not materially affected by detaching the kinocilium from the hair bundle and immobilizing it against the apical cellular surface with a microelectrode (*bottom trace*). *D*, A hair bundle bathed in standard saline solution containing 4 mM Ca^{2+} produced a twitch (*top trace*). After replacement of this solution with one containing 250 μM Ca^{2+}, the same bundle produced a twitch of similar magnitude but greater duration (*bottom trace*). In the presence of a Ca^{2+} concentration similar to that of endolymph, mechanical stimulation often produced oscillatory bundle movements at a frequency (here 65 Hz) similar to that at which saccular afferent fibers are tuned (Koyama et al., 1982). Stimulus fiber base displacements for *A*, *B*, *C*, and *D* were 130, 140, 300, and 143 nm, respectively; the fiber stiffnesses were 448, 353, 137, and 535 $\mu N \cdot m^{-1}$, respectively; the traces represent the averages of 12, 14–16, 10, and 10 responses, respectively.

the positive direction, usually appeared as an exaggeration of the bundle's passive deflection. The twitch's second phase was more prominent: motion in the direction of the stimulus was transiently interrupted by movement in the negative direction, against the applied force.

A mechanical twitch followed positively directed bundle movements in 164 hair cells of 399 studied in detail. Three observations linked the twitch with mechanoelectrical transduction. First, a twitch was observed only if a hair cell was capable of normal transduction, i.e., if it possessed an intact hair bundle, had a resting membrane potential below −45 mV, exhibited high sensitivity to small stimuli, and evinced adaptation. Second, a twitch ensued only after deflection of a hair bundle along its axis of mechanical sensitivity (Shotwell et al., 1981). Perpendicular stimulation did not evoke a twitch (Fig. 3*A*). Finally, no twitch occurred when transduction channels were blocked (Fig. 3*B*) by exposure of the bundle to the aminoglycoside antibiotic gentamycin (Kroese et al., 1989).

The twitch was produced by the stereocilia in a hair bundle, for the response persisted in bundles whose kinocilia had been disconnected from the stereocilia by microdissection (Hudspeth and Jacobs, 1979) and were held flat against the epithelial surface with microelectrodes (Fig. 3*C*). Twitching was not an aberrant response to the ionic environment ordinarily used in experimentation, in which hair cells were exposed to a saline solution containing 4 mM Ca^{2+}. A twitch could readily be evoked when a hair bundle was bathed in saline solution containing 250 μM Ca^{2+} (Fig. 3*D*), the concentration found in frog endolymph (Corey and Hudspeth, 1979).

Negatively directed stimulus components evoked twitches infrequently, in only 21 cells of the sample. Fourteen of these cells exhibited twitches in response to both positive and negative stimulus components (Fig. 4); the other seven displayed only negative twitches in association with negative stimulus components. When a twitch was elicited by a negatively directed bundle displacement, it usually followed a static offset of the bundle by ≥500 nm in the positive direction. Because responses to negative stimulus components were rarely encountered, the balance of the present study is devoted to analysis of twitches elicited by positive bundle motions.

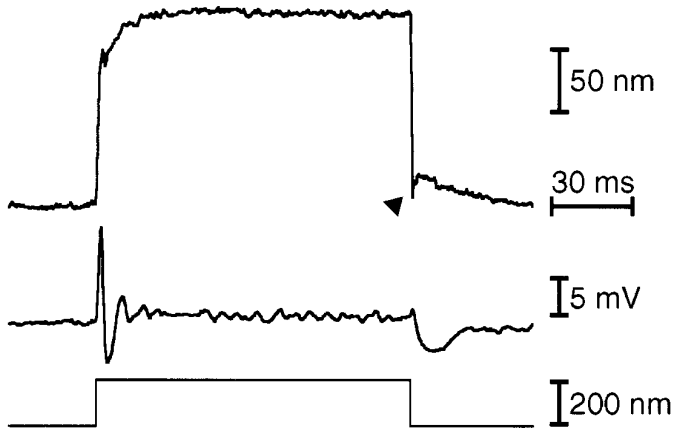

Figure 4. A twitch evoked by a negatively directed stimulus component. Driven by a 213 nm movement of the fiber's base (*bottom trace*), the hair bundle's movement (*top trace*) included both a positively directed twitch at the pulse's outset and a negatively directed twitch (*arrowhead*) at the pulse's conclusion. Unlike the initial twitch, the mechanical response at the pulse's end was not associated with a strong spike of depolarizing receptor potential (*middle trace*). The results from 10 stimuli were averaged. The fiber's stiffness was 283 $\mu N \cdot m^{-1}$; the cell's resting potential was −56 mV.

Dependence of the twitch on the amplitude and rate of hair bundle deflection

To characterize the twitch, we required a quantitative measure of the response's magnitude. We defined the amplitude of a twitch as the distance between the peak of the initial, positively directed motion and the greatest extent of the subsequent, negative excursion (Fig. 2*C*). A reasonable alternative measure would have been the distance between the positive peak deflection and the intercept of the bundle movement subsequent to the twitch extrapolated back to the rising phase of bundle deflection. However, because the time course of adaptation is not strictly exponential (Assad and Corey, 1992) and extrapolation is therefore complex, we elected to use the simpler definition of twitch amplitude. For data analysis and plotting, hair bundle displacement was scored as the distance from a bundle's resting position to the most negative position during a twitch.

Twitches occurred in response to positive bundle deflections as small as 5 nm. It is not certain whether lesser stimuli also elicited twitches; for averages of 10–16 experimental records, responses smaller than 1 nm were lost in the noise. When positive stimuli of progressively greater amplitude were applied to a hair bundle, the amplitude of the twitch grew with the bundle deflection (Fig. 5*A*). This relation was not monotonic: the twitch reached a maximal amplitude on hair bundle displacements of 13–48 nm, then declined with still larger stimuli (Fig. 5*B*). Similar relations were observed for a total of 24 hair bundles on which complete measurements were made; for this sample, the average bundle displacement at which the maximal twitch could be evoked was 34 ± 9 nm (mean ± SD). The greatest stimulus-evoked twitch observed from any bundle was 30 nm.

By varying the corner frequency of the low-pass filter for the stimulus fiber actuator, we investigated the twitch's sensitivity to the rate of bundle deflection. Slowing stimulation by increasing the rise time of bundle movement diminished and broadened the twitch (Fig. 6*A*). Moreover, as the bundle's rise time increased, the displacement required to evoke a maximal twitch also rose (Fig. 6*B*). Including the hair bundle whose response is illustrated, all of the 10 bundles studied in detail displayed similar sensitivities of twitching to the rate of stimulus rise.

Relation of twitch amplitude to hair bundle holding position

The twitch was sensitive to the position at which a bundle was maintained before stimulation. This holding position was adjusted by offsetting the base of the adherent stimulus fiber; the magnitude of the offset was determined from the motion required to re-center the displacement monitor over the bundle's new position. Bringing a stimulus fiber into contact with a hair bundle can move the bundle slightly and thus render the zero position of bundle offset somewhat uncertain. To minimize this problem, we used an eyepiece reticle to measure each hair bundle's position

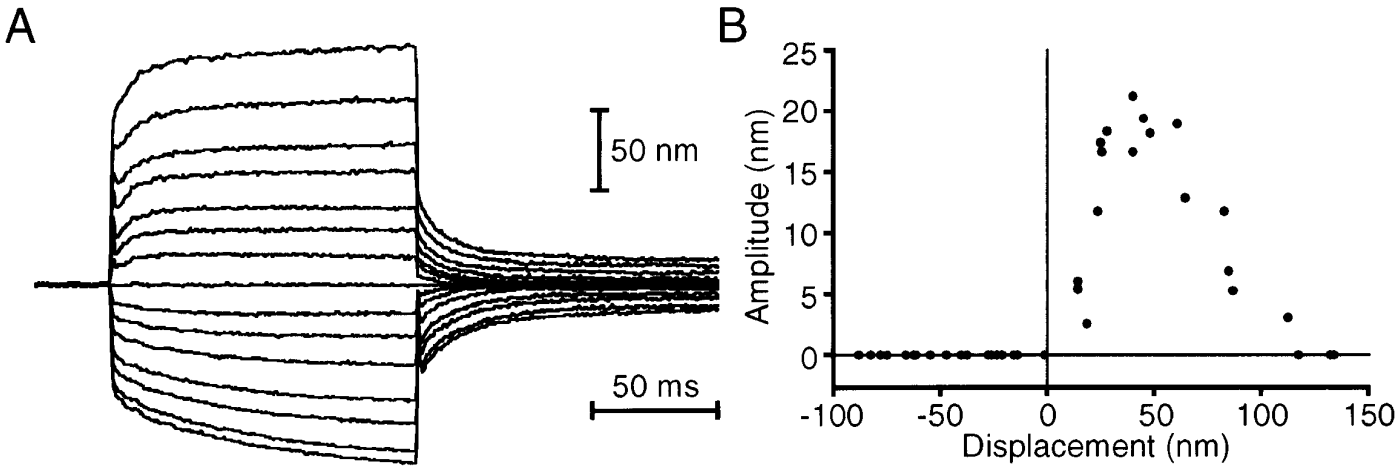

Figure 5. The twitch's dependence on hair bundle displacement, as determined by application of variable-amplitude displacement pulses to the base of a stimulus fiber. *A*, This bundle's superimposed responses showed that the twitch grew in amplitude with increasing bundle displacement for values up to ~40 nm; for greater bundle displacements, the twitch's amplitude progressively declined to zero. *B*, The twitch's amplitude is plotted as a function of hair bundle displacement. In *A*, 14 step displacements, each 400 msec in duration, were delivered to the fiber's base; the steps were uniformly spaced between and included −400 and 400 nm. An additional record was obtained in the absence of a displacement. The results from 10 stimulus wave trains were averaged; averaged responses of <1 nm, which did not significantly exceed the noise level, are plotted as zero. The data in *B* were obtained from the same hair bundle by three repetitions of the procedure used to obtain *A*. The fiber's stiffness was 293 $\mu N \cdot m^{-1}$.

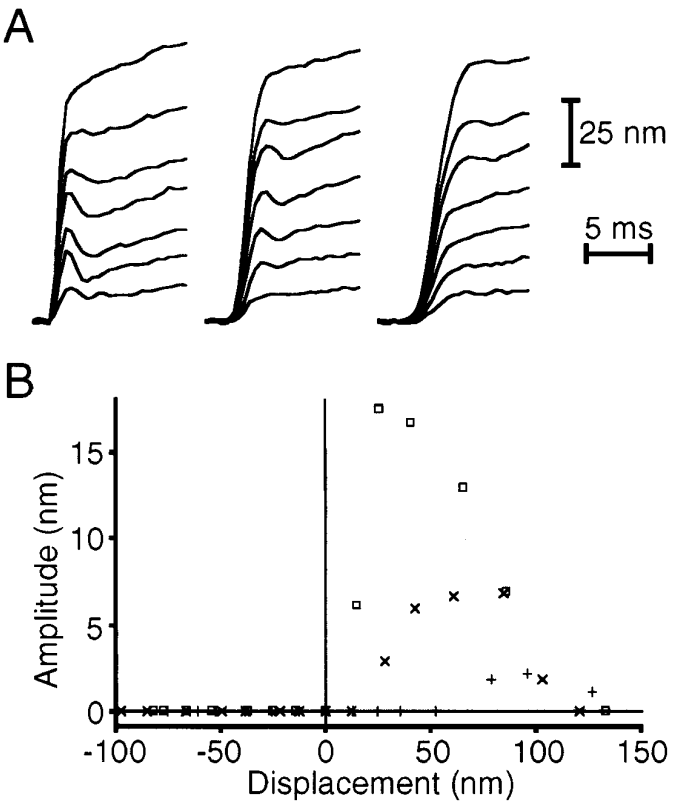

Figure 6. Effect of stimulus rise time on the amplitude and time course of twitches. *A*, Sets of variable-amplitude stimuli were delivered to a hair bundle, with each set low-pass-filtered at a different frequency. The twitch's duration increased and its amplitude declined with increasing rise time. The half-power frequencies of stimulus filtering were 500 Hz (*left panel*, averages of 10 presentations), 250 Hz (*middle panel*, averages of 9 presentations), and 150 Hz (*right panel*, averages of 8 presentations). Filtering at still higher frequencies did not materially change twitch durations or amplitudes from those observed for filtering at 500 Hz. Fiber-base excursions were varied from 57 to 400 nm in 57 nm increments; the fiber's stiffness was 293 $\mu N \cdot m^{-1}$. *B*, Twitch amplitude is plotted as a function of hair bundle displacement for the three families of variable-amplitude responses shown in *A*. Twitch amplitude decreased with greater rise time; in addition, the bundle displacement that elicited the largest twitch increased with the rise time. Because repetition of the stimuli elicited similar responses, it is improbable that fiber drift accounted for the observed results. The half-power frequencies of stimulus filtering were 500 Hz (□), 250 Hz (x), and 150 Hz (+).

before attachment of a fiber, then restored the bundle to that position before stimulation.

Even when elicited by identical stimuli, the amplitude and time course of a bundle's twitch changed substantially and reversibly between holding positions (Fig. 7*A*). A twitch could be evoked from a range of holding positions, usually between −350 and 300 nm; larger offsets in either direction suppressed the response. Because adaptation by the mechanoelectrical transduction process is limited to a similar range, this effect may reflect the influence of the extent spring thought to be associated with each transduction element (Shepherd and Corey, 1994).

Twitch amplitudes fell into a bell-shaped distribution about the bundle's undisturbed resting position (Fig. 7*B*). For 35 hair cells, we found that the twitch could grow into several cycles of damped oscillation (Fig. 7*C*). This behavior could often be accentuated by adjustment of the bundle's offset position.

Fatigue, potentiation, and repriming of the twitch

To determine whether the twitch exhibits fatigue or a refractory period, we stimulated hair bundles twice in succession and varied the interval between the pulse onsets. For 8 of 11 bundles, the twitch elicited by the second pulse was distinctly smaller than the first response (Fig. 8*A*). This phenomenon was most prominent for stimulus intervals of <20 msec. Six bundles exhibited a potentiation of the second twitch, which was most pronounced for stimulus intervals exceeding 30 msec and followed a time course similar to that of adaptation (Fig. 8*B*) (Howard and Hudspeth, 1987a). Five bundles exhibited both short-interval fatigue and long-interval potentiation; one bundle exhibited only potentiation, three bundles solely fatigue. Two bundles showed no change in the magnitude of the second twitch relative to that of the first.

A bundle's ability to twitch during the positively directed return from a negative displacement increased with the duration of the deflection (Fig. 9*A*). The time course over which the twitch reached its greatest size depended on the amplitude of the stimulus: the smaller the bundle's negative displacement, the less time was required for the twitch to attain its maximal amplitude (data not shown). For displacements of ~50 nm, the twitch's amplitude increased with a time course again resembling that of adaptation (Fig. 9*B*).

Forces associated with the twitch

A fast displacement clamp system permitted us to measure the forces exerted by a hair bundle during twitches in eight hair cells. These forces were determined from the flexion of the stimulus fiber required to effect and maintain a bundle's deflection in response to a displacement command pulse (Fig. 10*A*). To displace a bundle in the positive direction, the fiber initially worked against the forces due to the elastic reactance of the hair bundle and the viscous drag on the bundle and fiber. During a maintained displacement, the force produced by the fiber gradually declined during the adaptation process (Jaramillo and Hudspeth, 1993).

The force transient recorded immediately after a positive bundle displacement, and hence associated with twitching, was distinctly biphasic (Fig. 10*B*); this was especially apparent for twitches that had prolonged rising phases. The bundle first produced a positively directed force, i.e., a force in the direction of the stimulus. Within a few milliseconds, this component was followed by a larger force in the opposite direction, against the applied force. Comparison of the forces exerted under displacement clamp conditions with the twitch elicited from the same bundle under base movement conditions indicated that the twitch's positive phase coincided with the positively directed component of bundle force (Fig. 10*C*). The second, negatively directed component of the twitch corresponded to a force exerted by the bundle in the negative direction.

Relation of the twitch to mechanoelectrical transduction

The twitch was consistently associated with robust mechanoelectrical transduction. During positive stimulation, a large transient in the depolarizing receptor potential coincided with the hair bundle's twitch (Fig. 2*A*). Twitches evoked by negative stimuli were accompanied by negative receptor potentials (Fig. 4); these hyperpolarizations did not, however, exhibit the fast time course and large magnitude typical of responses to positive stimuli. Cells whose hair bundles produced distinct twitches, at least 3 nm in amplitude, yielded an average maximal receptor potential of 9.1 ± 6.9 mV (mean ± SD, $n = 164$ cells). By contrast, morphologically

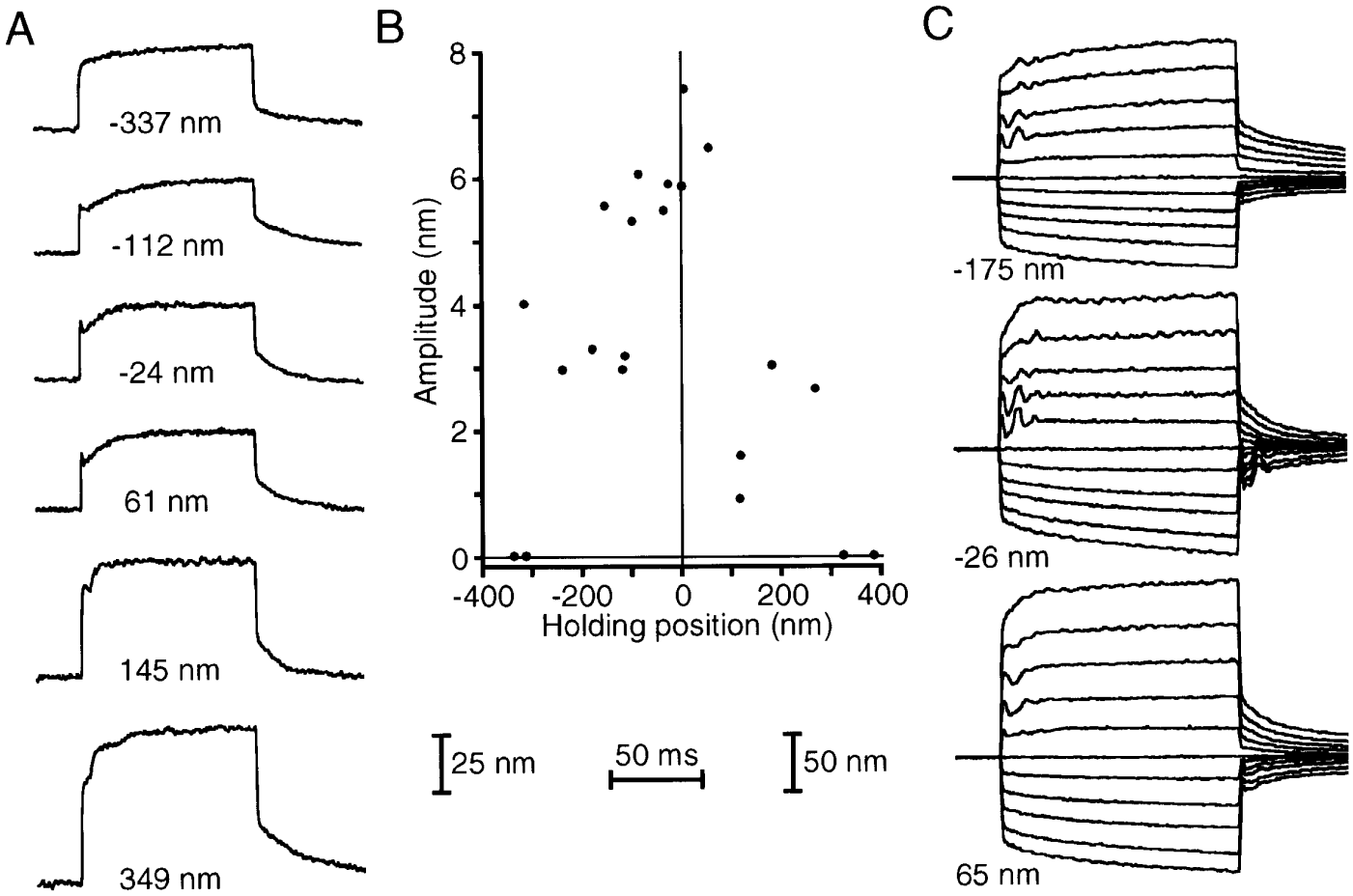

Figure 7. The effect of holding position on twitches. *A*, By application of static offsets to the attached fiber, a hair bundle's holding position was adjusted by the amounts shown *below* the traces. Identical, 140 nm displacement pulses were then applied to the fiber's base. Although twitches occurred for a range of holding positions around the bundle's resting position, they were suppressed by holding the bundle far in the positive or negative direction. Each trace is the average response to 8–10 stimulus presentations; the fiber's stiffness was 272 $\mu N \cdot m^{-1}$. *B*, The mean twitch amplitudes of responses resulting from 140 nm stimulus pulses are plotted as a function of the bundle's holding position. No twitches occurred from holding positions still more positive or negative than those shown. *C*, Adjustment of a hair bundle's holding position caused twitches to become several cycles of damped mechanical oscillation. The bundle offsets for the three response families are shown to the *bottom left* of the respective records. Traces are the averages of 10–13 wavetrains of fiber-base excursions that were uniformly spaced between −300 and 300 nm. The fiber's stiffness was 623 $\mu N \cdot m^{-1}$. The *distance calibration bar* at the *left* applies to *A*, the *bar* at the *right* applies to *C*, and the *temporal calibration bar* (*middle*) applies to both.

similar hair cells lacking twitches displayed a mean peak response of 3.8 ± 3.5 mV ($n = 235$). By a one-tailed t test, the former is a significantly greater value ($p < 10^{-16}$). In many instances, the membrane potential exhibited oscillations subsequent to stimulation (Fig. 11*A*), a manifestation of the electrical resonance characteristic of the bullfrog's saccular hair cells (Lewis and Hudspeth, 1983; Hudspeth and Lewis, 1988a,b). Such oscillations were not, however, uniformly associated with bundle twitching.

To examine the displacement dependencies of the twitch and of mechanoelectrical transduction, we stimulated a cell with positive displacement pulses of various sizes and measured the twitch's amplitude in relation to that of the receptor potential (Fig. 11*B*). The twitch reached its maximal size with bundle displacements considerably smaller than those of 100–150 nm that saturated the electrical response. The twitch peaked at approximately the midpoint of the range of mechanical sensitivity, the bundle position at which about half of the transduction channels were open.

The receptor potential provided a somewhat distorted index of mechanoelectrical transduction, because the electrical response was filtered by the membrane's time constant and augmented by electrical resonance. We therefore related the amplitude of the twitch to that of the transduction current, which we estimated from the initial slope of the receptor potential's rising phase. The twitch amplitude was greatest near the point at which this slope changed most rapidly with bundle displacement (Fig. 11*C*). To emphasize this point, we plotted the twitch's amplitude against the rate at which the receptor potential's slope changed as a function of bundle displacement. Within the experimental uncertainty, the two responses were linearly related (Fig. 11*D*). Taken together, these results confirmed that the twitch peaked at bundle displacements for which the mechanoelectrical transduction process was most sensitive.

Spontaneous hair bundle twitching

Twenty-three hair bundles exhibited spontaneous twitches; 20 of these produced positively directed movements (Fig. 12*A*), the balance negative twitches. Although it was difficult to distinguish small twitches from Brownian motion, the amplitudes of spontaneous twitches ranged up to 42 nm. The clearly identifiable spontaneous movements had durations of 3–10 msec.

Spontaneous hair bundle motions varied widely in their regu-

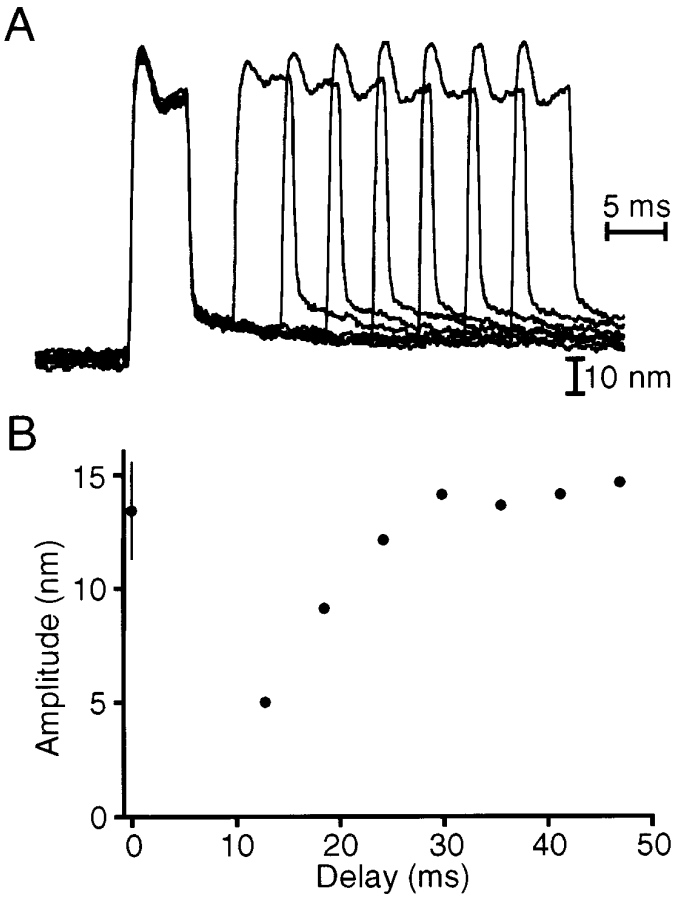

Figure 8. Fatigue and potentiation of the twitch response. *A*, Seven pairs of equal-amplitude and equal-duration displacement pulses were delivered to a stimulus fiber's base with various delays between the pulses' commencements. The twitch ensuing from the second stimulus was partially suppressed for the smallest intervals, then became slightly exaggerated with larger intervals. The delay between successive pairs of pulses was 150 msec; the results of 10 wave trains were averaged. The fiber of stiffness 535 $\mu N \cdot m^{-1}$ was displaced by 200 nm at its base. The displacement monitor's output was filtered at 7 kHz and sampled by the computer at 14 kHz. *B*, The amplitude of the twitch elicited by the second pulse grew with the delay between the pulses' onsets. The mean of the control response is shown with its SD.

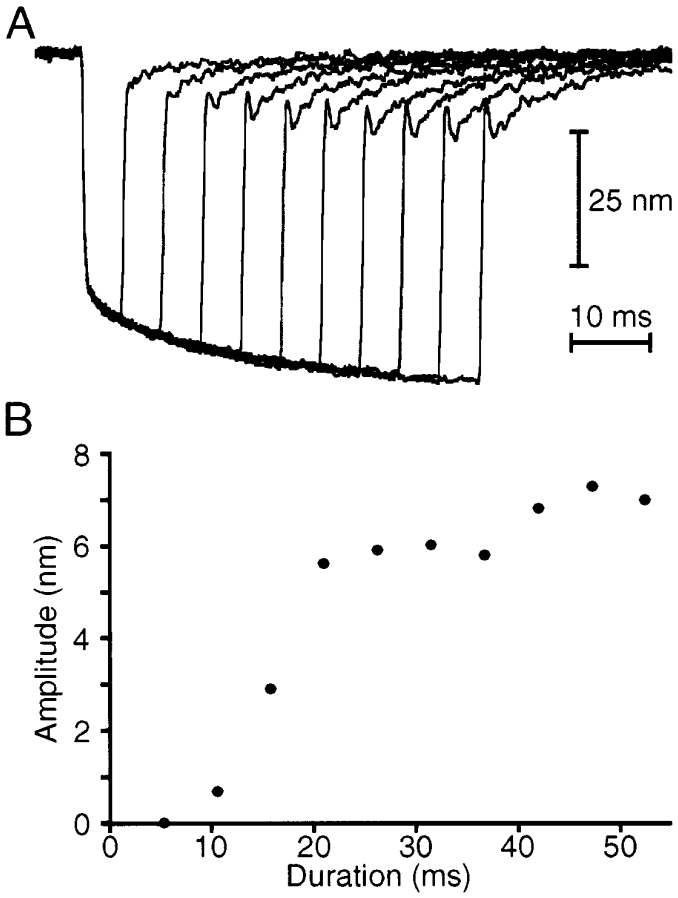

Figure 9. Development of the twitch during negative stimulation. *A*, A hair bundle was subjected to 10 stimuli of equal size, a fiber-base displacement of −300 nm, but differing durations. The amplitude of the twitch at the displacement's conclusion grew monotonically with the duration of the stimulus. The delay between successive stimuli was 300 msec; the results of 14 stimulus wavetrains were averaged. The displacement monitor's output was filtered at 3.5 kHz and communicated to the computer at 10 kHz. The fiber's stiffness was 310 $\mu N \cdot m^{-1}$. *B*, A plot of twitch amplitudes from *A* against the durations of negative pulses demonstrates the gradual development of the capacity for twitching. Note that the time course of twitch capacitation approximately corresponds to that of mechanical adaptation.

larity. Like those observed earlier from hair bundles of the turtle's basilar papilla (Crawford and Fettiplace, 1985) and the frog's sacculus (Howard and Hudspeth, 1987a), some movements were essentially sinusoidal. Even when spontaneous twitching was not regularly periodic, the average number of spikes in a given time period varied systematically with a hair bundle's holding position. Spontaneous twitches occurred over a range of bundle holding positions, with a bell-shaped distribution of twitching rate centered somewhat positive to the bundle's resting position. The rate of spontaneous twitching during brief bundle displacements showed a similar sensitivity to bundle position (Fig. 12*B*). After a positive bundle deflection, the propensity to twitch transiently increased, then declined to its resting level. Twitching was diminished during maintained negative bundle displacements; the more negative the static displacement, the longer it took for the rate of twitching to increase to the resting level.

Spontaneous twitches were associated with stimulation of the transduction elements, because transient membrane depolarizations coincided with positive bundle movements (Fig. 12*C*).

The well defined time course of spontaneous twitches facilitates calculation of the mechanical work performed by a bundle in their production. When a bundle with a drag coefficient of 200 $nN \cdot sec \cdot m^{-1}$ (Howard and Hudspeth, 1988) produced a 25 nm, triangle-wave twitch 5 msec in total duration (Fig. 12*A*), the energy dissipated against viscous drag was ~100 zJ (a zeptojoule is 10^{-21} J). By way of comparison, this quantity approximately equals the free-energy change associated with the hydrolysis of two ATP molecules or the movement of four Ca^{2+} ions across the cell's membrane. If the elastic work done during the twitch's rising phase was not recovered during the falling phase, the energy used in performing work against the stiffnesses of the bundle and stimulus fiber exceeded 900 zJ, the equivalent of 20 molecules of ATP or the transmembrane flux of 40 Ca^{2+} ions.

DISCUSSION

Varieties of mechanical signals in the hair bundle

In conjunction with previous investigations, the present results indicate that a hair bundle exhibits at least four distinct forms of

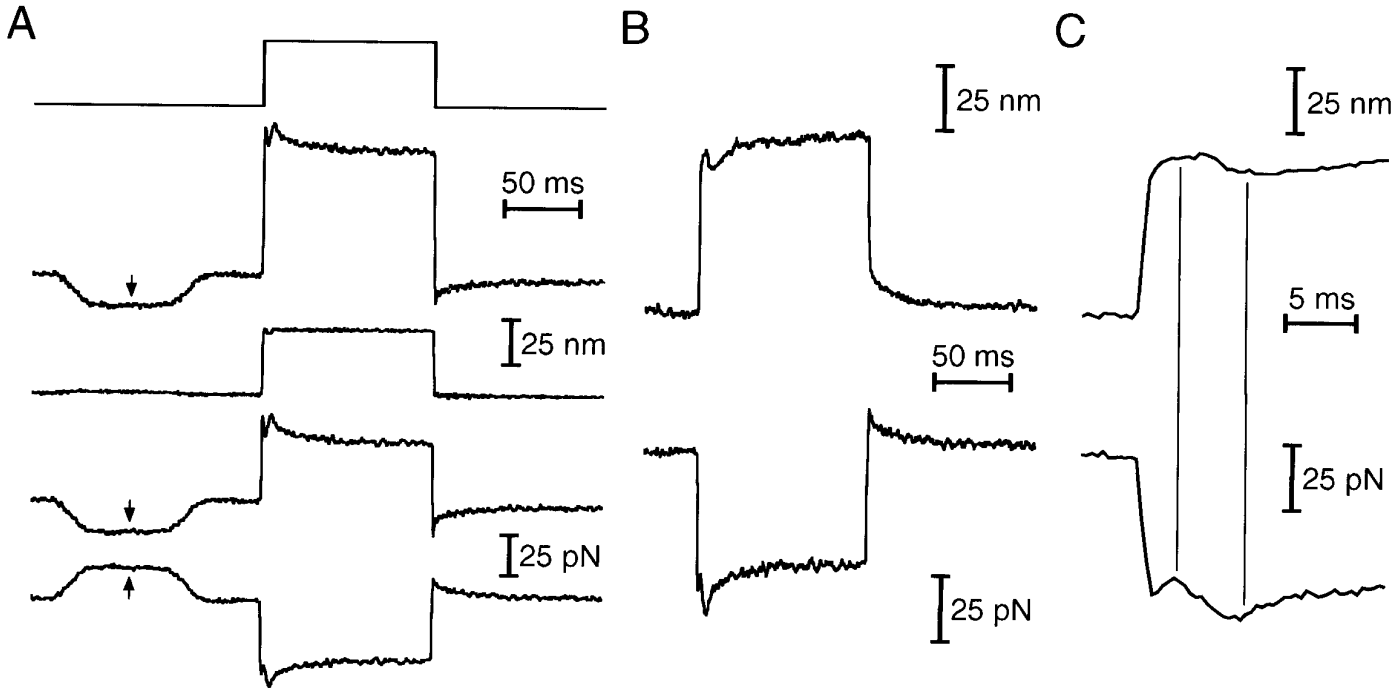

Figure 10. Displacement clamp measurement of the twitch force. *A*, When a pulse displacement command (*top trace*) was applied to the clamp system, the fiber's base underwent a convoluted excursion (*second trace*) while effecting the commanded hair bundle displacement (*third trace*). The total force exerted by the fiber (*fourth trace*) was determined by multiplication of its flexion, the difference between the second and third traces, by its calibrated stiffness of 951 $\mu N \cdot m^{-1}$. The hydrodynamic damping force on the fiber and bundle, which produced transients at the onset and conclusion of the displacement pulse, was calculated as the product of the fiber tip's instantaneous velocity and the summed drag coefficients of the fiber and bundle (Howard and Hudspeth, 1988). Subtraction of this force component yielded the force exerted by the bundle (*fifth trace*), which was directed opposite to that produced by the fiber. The *downward deflections* at the *left* of three traces (*arrows*) demonstrate the displacement clamp's effectiveness. When the photodiode pair in the displacement monitor was subjected to a 20 μm calibration pulse, the clamp circuit produced a compensatory, 20 nm movement of the fiber's tip. The record of bundle motion consequently shows almost no signal, while the records of fiber base displacement and the force traces display the response. These records indicate that the clamp system was, in this instance, 95% effective at controlling movement of the fiber's tip. *B*, *C*, Comparison of the same hair bundle's responses under base movement conditions (*top traces*) and displacement clamp conditions (*bottom traces*) demonstrates the relation between the twitch and the associated bundle forces on two time scales. The positively directed initial component of the twitch is associated with a positively directed force exerted by the bundle (*left vertical line* in *C*). The twitch's second, negatively directed component corresponds to a negatively directed bundle force (*right vertical line* in *C*). The fiber's damping constant was 79.5 $nN \cdot sec \cdot m^{-1}$, and its base displacement for the *top traces* of *B* and *C* was 120 nm. The traces in *A* represent the averages of five results; those in *B* and *C* are the averages of 10 results.

mechanical responsiveness. First, a bundle displays linear elasticity evoked by stimuli of any duration. A bundle's passive stiffness, which depends on the length and number of constituent stereocilia, is 300–4000 $\mu N \cdot m^{-1}$ (Flock and Strelioff, 1984a,b; Crawford and Fettiplace, 1985; Howard and Ashmore, 1986; Howard and Hudspeth, 1987a,b, 1988; Russell et al., 1992). The stiffness is greatest for forces applied along the bundle's axis of symmetry and mechanosensitivity (Fig. 3*A*) (Howard and Hudspeth, 1987a). About half of the work done in displacing a bundle along that axis contributes to transduction-channel gating (Howard et al., 1988), with the balance devoted to flexion of the actin fascicles at the basal pivots of the stereocilia (Crawford and Fettiplace, 1985; Howard and Ashmore, 1986).

A second mechanical response of the hair bundle reflects the gating of mechanoelectrical transduction channels. Within a range of positions near the bundle's resting point, the bundle's stiffness is less than that when the bundle is displaced more extensively in the positive or negative direction (Howard and Hudspeth, 1988; Russell et al., 1992; van Netten and Khanna, 1994). This phenomenon, termed gating compliance, reflects the fact that gating springs bear a significant fraction of the tension in a bundle; as channels flicker between their open and closed states, the time-averaged gating-spring tension declines, and a bundle consequently becomes less stiff (for review, see Hudspeth, 1992; Markin and Hudspeth, 1995).

A third, time-dependent change in the hair bundle's properties is associated with adaptation of mechanoelectrical transduction to sustained bundle deflection. After the initial movement reflecting its passive elasticity, a bundle displaced by a flexible fiber gradually relaxes toward its steady-state position (Fig. 2) (Howard and Hudspeth, 1987a; Russell et al., 1989); the time constant of this relaxation, ~25 msec, corresponds to that for adaptation of the electrical response (Eatock et al., 1987; Crawford et al., 1989; Assad and Corey, 1992). Maintaining a bundle's deflection constant with a displacement clamp system demonstrates that the bundle exerts a force that declines with similar kinetics (Fig. 10) (Jaramillo and Hudspeth, 1993). These mechanical measurements reflect an adjustment of the bundle's chord stiffness during adaptation (Hudspeth, 1992) consistent with the re-setting of gating-spring tension by a myosin-based motor (for review, see Hudspeth and Gillespie, 1994). Consistent with this model, myosin Iβ occurs near the stereociliary tips (Gillespie et al., 1993), the site of transduction (Hudspeth, 1982; Jaramillo and Hudspeth, 1991; Denk et al., 1995; Lumpkin and Hudspeth, 1995). Moreover, adaptation is blocked by nucleotide analogs that interfere with myosin's ATPase cycle (Gillespie and Hudspeth, 1993) and by

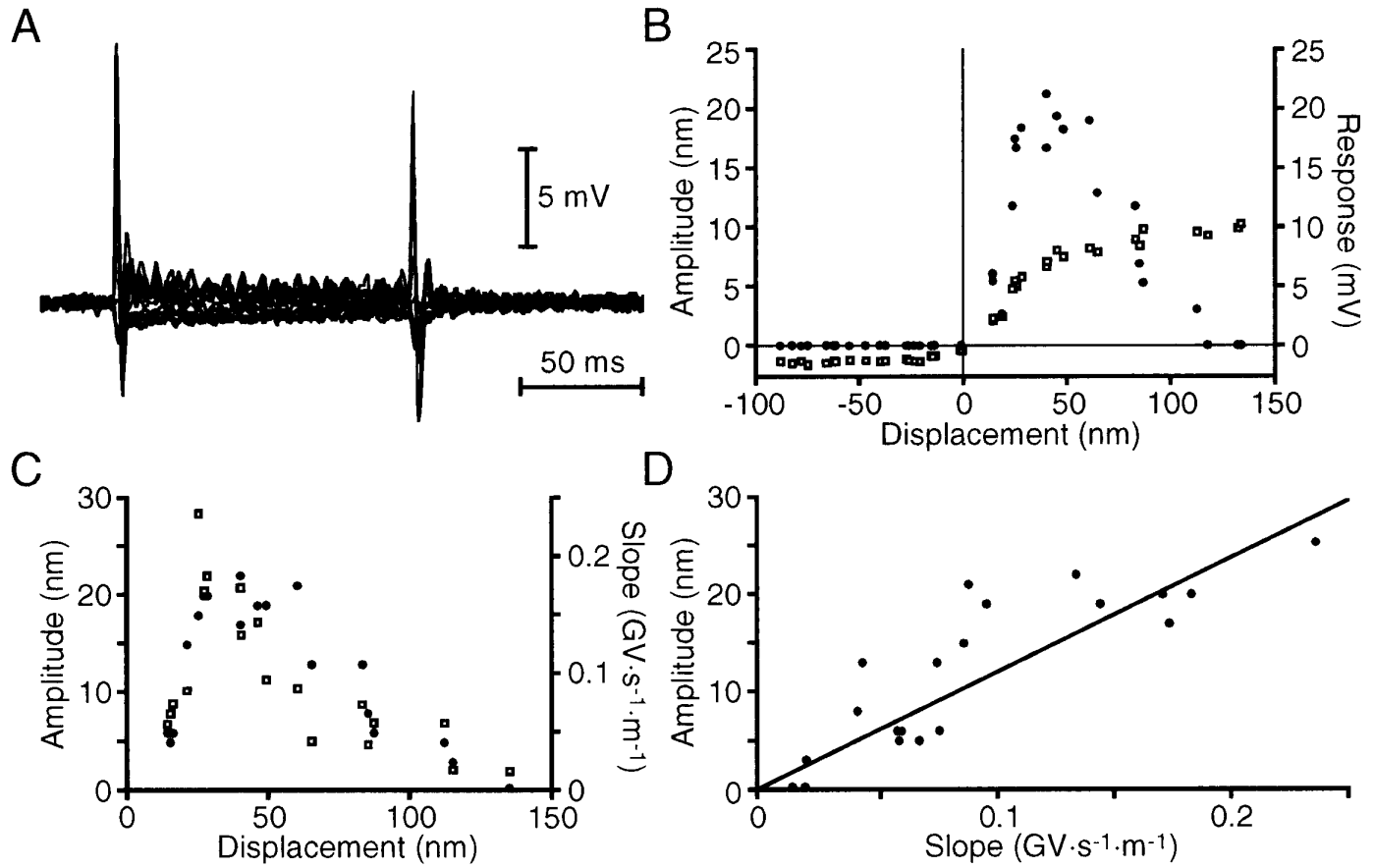

Figure 11. Relation of twitches to the sensitivity of mechanoelectrical transduction. *A*, Variable-amplitude stimuli, applied to the base of a stimulus fiber, the tip of which was attached to a hair bundle, elicited a family of receptor potentials. The corresponding mechanical traces for this cell occur in Figure 5*A*. *B*, While the amplitude of the receptor potential (□) grew monotonically with the stimulus size, the twitch's amplitude (●) peaked for a bundle displacement near 40 nm. *C*, The twitch's amplitude (●) is plotted against bundle displacement for another hair cell. As a measure of the sensitivity of mechanoelectrical transduction, the plot includes the derivative of the receptor potential's slope as a function of bundle displacement (□). The initial slope of the receptor potential was determined by measuring the increment in electrical response between successive points separated by a 400 μsec sampling interval. *D*, The relation between the estimated sensitivity of mechanoelectrical transduction and twitch amplitude is approximately linear; the minimal squared error line through the origin is associated with a correlation coefficient $r = 0.74$. *A* represents the results from 15 step displacements uniformly spaced from −400 to 400 nm; the results from 10 stimulus wave trains were averaged. The fiber's stiffness was 293 $\mu N \cdot m^{-1}$, and the cell's resting potential was −63 mV.

calmodulin inhibitors that interrupt Ca^{2+} modulation of myosin's activity (Walker and Hudspeth, 1996).

The present results delineate a fourth type of mechanical response from the hair bundle, rapid twitching evoked by stimulation. Movements of this sort have previously been observed from hair bundles of the bullfrog's sacculus (Howard and Hudspeth, 1987a,b, 1988; Jaramillo et al., 1990). Mechanically evoked bundle motions have also been seen in the turtle's basilar papilla (Crawford and Fettiplace, 1985); perhaps because relatively long stimulus fibers limited the frequency response of those measurements, however, twitches were not reported in that study.

In the present experiments, abrupt deflection of a bundle along its axis of mechanical sensitivity was followed immediately by an active movement comprising at least two phases, the first in the direction of the stimulus and the second opposite it. Simultaneous measurements of the receptor potential revealed an associated depolarizing transient. Furthermore, the twitch's magnitude was maximal over the range of stimulus displacements for which transduction was most sensitive. Because twitching was inhibited when transduction channels were blocked with gentamicin (Fig. 3*B*), and because it could not be elicited by stimulation perpendicular to the bundle's axis of mechanosensitivity (Fig. 3*A*), the twitch response seems intimately related to the mechanoelectrical transduction process. This linkage is strengthened by the observation that a bundle's capacity to twitch accumulated with a time course characteristic of adaptation (Figs. 8*B*, 9*B*). In addition, the range of bundle positions over which a twitch could be elicited (Fig. 7*B*) resembled that over which adaptation is effective (Shepherd and Corey, 1994). The adaptation process therefore appears to poise the twitch-producing apparatus in readiness to make active movements.

Possible mechanisms of the twitch

Two simple models offer insight into the twitch's origin. Both suppose that the twitch is caused by a brief decrease in average gating-spring tension followed immediately by a transient increase. The results of our displacement clamp experiments support this notion: the twitch's two phases correspond to, respectively, a decrease and an increase in the force exerted by the bundle against the stimulus fiber (Fig. 10).

The first model is based on the activity of mechanoelectrical transduction channels (Howard and Hudspeth, 1988; Jaramillo et al., 1990). If a large fraction of these channels were to open

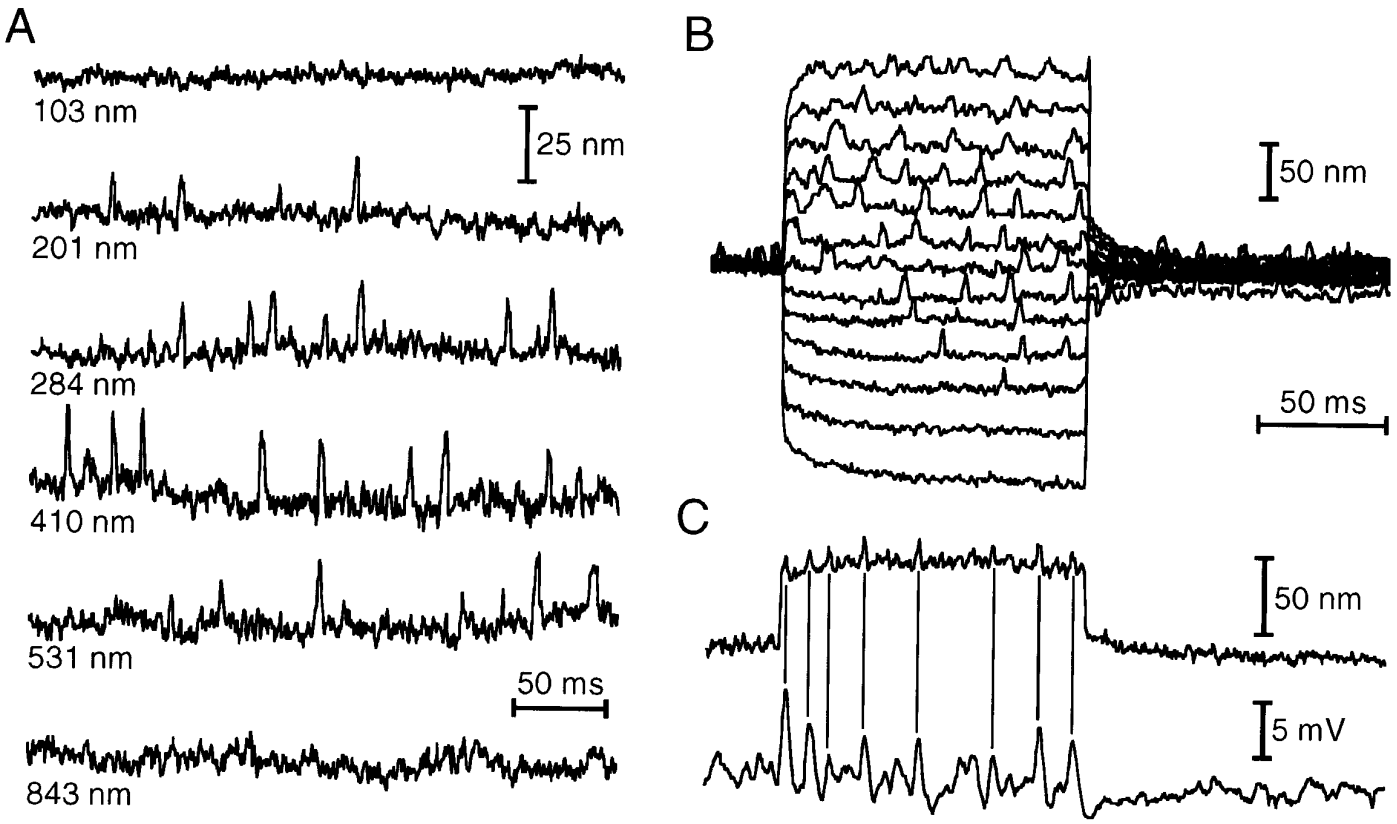

Figure 12. Spontaneous twitching by hair bundles. *A*, Rapid, positively directed twitches of amplitudes as great as 30 nm were clearly distinct from the hair bundle's RMS Brownian motion of ~2 nm. The propensity to twitch depended on a bundle's holding position, which is shown to the *lower left* of each trace. *B*, The same bundle's rate of twitching was also sensitive to brief bundle displacements. Especially during negative displacement pulses, twitching required tens of milliseconds to resume. The bundle offsets were produced by 13 fiber base excursions that were uniformly varied in amplitude from −350 to 350 nm. The fiber's stiffness was 310 $\mu N \cdot m^{-1}$. *C*, In another hair cell, spontaneous twitching of the hair bundle (*top trace*) was roughly synchronous with transient membrane depolarizations (*bottom trace*); the electrical responses may have been slightly delayed by the filtering effect of the membrane's time constant. The responses were elicited by a 60 nm base displacement of a fiber of stiffness 753 $\mu N \cdot m^{-1}$; the cell's resting potential was −45 mV. The time calibrations of *B* and *C* are identical.

simultaneously just after a positive bundle deflection, the average gating-spring tension would decrease as the channels' gates assumed their open conformation. Concerted channel closing would conversely increase the tension in the gating springs and pull the bundle in the negative direction. If a transduction channel occurs at one end of each tip link, the conformational change associated with the opening of its gate is 4 nm (Howard and Hudspeth, 1988); if there are channels at each end of a link, the estimated motion is 2 nm (Denk et al., 1995). Considering the geometrical gain of the bundle, 0.14 (Howard and Hudspeth, 1988), concerted channel gating could in either case move an unrestrained bundle ~30 nm, which is near the amplitude of the largest evoked twitches that we observed.

The bundle's adaptation motors provide an alternative means of effecting a rapid decrease and increase in gating-spring tension. It is plausible that myosin molecules at the insertional plaque respond to a stretch stimulus, such as bundle deflection, by tilting their heads (Huxley and Simmons, 1971) and thus reducing gating-spring tension. Such a reversal of the power stroke can proceed rapidly, with a rate constant of 1500 sec^{-1} in muscle fibers (Lombardi et al., 1995). A subsequent power stroke would increase the gating-spring tension, pulling the bundle back in the negative direction. Given a power stroke of ~11 nm (for review, see Huxley, 1990) and the bundle's geometrical gain, synchronous rocking of myosin heads could move an unrestrained bundle as much as 80 nm.

On the basis of either of these models, the sensitivity of mechanoelectrical transduction should be proportional to twitch magnitude. Our results (Fig. 11*D*) are consistent with this prediction, but a more direct assessment of the transduction current, under voltage-clamp conditions, will be necessary before a firm conclusion can be drawn. Such experiments should also differentiate between the two models. By the channel-gating model, the time course of the transduction current should follow that of the twitch's rising and falling components. The gates of transduction channels would be required, not only to close despite elevated gating-spring tension, but also to further augment this tension in an energy-requiring process. On the other hand, the adaptation motor model suggests that gating-spring tension should be increased, and channels should therefore remain open while motors pull the bundle back in the negative direction. Of course, the twitch's mechanism may be more complicated than either of the two models described above: transduction-channel gating and myosin-head tilting may operate in combination, with contributions from other hair bundle constituents as well.

Implications for amplification of inputs by hair cells

While producing a twitch movement against an elastic stimulus fiber and viscous drag, a hair bundle must perform mechanical work. The twitch therefore signals an active process capable of dissipating energy, presumably that derived from hydrolysis of

ATP or from an ionic gradient. This behavior is of interest in light of the demonstrated amplificatory capacity of various auditory receptor organs. In the mammalian cochlea, for example, amplification is a nonlinear process that increases sensitivity to small stimuli and improves frequency selectivity (for review, see Ruggero, 1992). Outer hair cells are thought to effect amplification by voltage-driven contractions of their somata (for review, see Dallos, 1992). Our results indicate that evoked hair-bundle motility is also associated with increased sensitivity of transduction (Fig. 11). Bundle twitching might therefore enhance the responsiveness of hair cells in auditory and vestibular receptor organs (Howard and Hudspeth, 1988) (for review, see Hudspeth, 1989), perhaps including the mammalian cochlea.

Intense amplification of mechanical signals likely underlies spontaneous otoacoustical emissions (for review, see Probst, 1990). Hair bundles exhibit spontaneous twitching of an amplitude well in excess of Brownian motion (Fig. 12) (see also Crawford and Fettiplace, 1985; Howard and Hudspeth, 1987a; Denk et al., 1989); it is therefore possible that bundles produce spontaneous otoacoustical emissions.

To participate in amplification and otoacoustical emissions, hair bundle motility would be required to accentuate the motion of accessory structures such as tectorial and basilar membranes. At least in the sacculus, hair bundles are rigid enough to move the overlying otolithic membrane (Benser et al., 1993); if they occurred simultaneously in numerous cells, the observed hair bundle twitches could produce sufficient force to displace this accessory structure. Although the stiffnesses of the cochlea's tectorial and basilar membranes remain uncertain, they may resemble that of the otolithic membrane (Gummer et al., 1981). If so, twitches or oscillations by the hair bundles of outer hair cells could affect basilar membrane movement and might thus contribute to the cochlea's sensitivity and sharpness of tuning.

REFERENCES

Art JJ, Crawford AC, Fettiplace R (1986) A method for measuring cellular movements less than the wavelength of light. J Physiol (Lond) 371:18P.

Assad JA, Corey DP (1992) An active motor model for adaptation by vertebrate hair cells. J Neurosci 12:3291–3309.

Benser ME (1995) Characterization of active hair-bundle motion and its effect on the mechanics of organs of the acousticolateralis system. PhD thesis, University of Texas at Arlington.

Benser ME, Issa NP, Hudspeth AJ (1993) Hair-bundle stiffness dominates the elastic reactance to otolithic-membrane shear. Hear Res 68:243–252.

Corey DP, Hudspeth AJ (1979) Response latency of vertebrate hair cells. Biophys J 26:499–506.

Corey DP, Hudspeth AJ (1983) Kinetics of the receptor current in bullfrog saccular hair cells. J Neurosci 3:962–976.

Crawford AC, Fettiplace R (1985) The mechanical properties of ciliary bundles of turtle cochlear hair cells. J Physiol (Lond) 364:359–379.

Crawford AC, Evans MG, Fettiplace R (1989) Activation and adaptation of transducer currents in turtle hair cells. J Physiol (Lond) 419:405–434.

Dallos P (1992) The active cochlea. J Neurosci 12:4575–4585.

Denk W, Webb WW (1992) Forward and reverse transduction at the limit of sensitivity measured by correlating electrical and mechanical fluctuations in frog saccular hair cells. Hear Res 60:89–102.

Denk W, Webb WW, Hudspeth AJ (1989) Mechanical properties of sensory hair bundles are reflected in their Brownian motion measured with a laser differential interferometer. Proc Natl Acad Sci USA 86:5371–5375.

Denk W, Holt JR, Shepherd GMG, Corey DP (1995) Calcium imaging of single stereocilia in hair cells: localization of transduction channels at both ends of tip links. Neuron 15:1311–1321.

Eatock RA, Corey DP, Hudspeth AJ (1987) Adaptation of mechanoelectrical transduction in hair cells of the bullfrog's sacculus. J Neurosci 7:2821–2836.

Flock Å, Strelioff D (1984a) Graded and nonlinear mechanical properties of sensory hair cells in the mammalian hearing organ. Nature 310:597–599.

Flock Å, Strelioff D (1984b) Studies on hair cells in isolated coils from the guinea pig cochlea. Hear Res 15:11–18.

Gillespie PG, Hudspeth AJ (1993) Adenine nucleoside diphosphates block adaptation of mechanoelectrical transduction in hair cells. Proc Natl Acad Sci USA 90:2710–2714.

Gillespie PG, Wagner MC, Hudspeth AJ (1993) Identification of a 120 kD hair-bundle myosin located near stereociliary tips. Neuron 11:581–594.

Gittes F, Mickey B, Nettleton J, Howard J (1993) Flexural rigidity of microtubules and actin filaments measured from thermal fluctuations in shape. J Cell Biol 120:923–934.

Gummer AW, Johnstone BM, Armstrong NJ (1981) Direct measurement of basilar membrane stiffness in the guinea pig. J Acoust Soc Am 70:1298–1309.

Howard J, Ashmore JF (1986) Stiffness of sensory hair bundles in the sacculus of the frog. Hear Res 23:93–104.

Howard J, Hudspeth AJ (1987a) Mechanical relaxation of the hair bundle mediates adaptation in mechanoelectrical transduction by the bullfrog's saccular hair cell. Proc Natl Acad Sci USA 84:3064–3068.

Howard J, Hudspeth AJ (1987b) Adaptation of mechanoelectrical transduction in hair cells. In: Sensory transduction (Hudspeth AJ, MacLeish PR, Margolis FL, Wiesel TN, eds), pp 138–145. Geneva: Fondation pour l'Etude du Système Nerveux Central et Périphérique.

Howard J, Hudspeth AJ (1988) Compliance of the hair bundle associated with gating of mechanoelectrical transduction channels in the bullfrog's saccular hair cell. Neuron 1:189–199.

Howard J, Roberts WM, Hudspeth AJ (1988) Mechanoelectrical transduction by hair cells. Annu Rev Biophys Biophys Chem 17:99–124.

Hudspeth AJ (1982) Extracellular current flow and the site of transduction by vertebrate hair cells. J Neurosci 2:1–10.

Hudspeth AJ (1989) How the ear's works work. Nature 341:397–404.

Hudspeth AJ (1992) Hair-bundle mechanics and a model for mechanoelectrical transduction by hair cells. In: Sensory transduction (Corey DP, Roper SD, eds), pp 357–370. New York: Rockefeller UP.

Hudspeth AJ, Corey DP (1978) Controlled bending of high-resistance glass microelectrodes. Am J Physiol 234:C56–C57.

Hudspeth AJ, Gillespie PG (1994) Pulling springs to tune transduction: adaptation by hair cells. Neuron 12:1–9.

Hudspeth AJ, Jacobs R (1979) Stereocilia mediate transduction in vertebrate hair cells. Proc Natl Acad Sci USA 76:1506–1509.

Hudspeth AJ, Lewis RS (1988a) Kinetic analysis of voltage- and ion-dependent conductances in saccular hair cells of the bull-frog, *Rana catesbeiana*. J Physiol (Lond) 400:237–274.

Hudspeth AJ, Lewis RS (1988b) A model for electrical resonance and frequency tuning in saccular hair cells of the bull-frog, *Rana catesbeiana*. J Physiol (Lond) 400:275–297.

Huxley AF, Simmons RM (1971) Proposed mechanism of force generation in striated muscle. Nature 233:533–538.

Huxley HE (1990) Sliding filaments and molecular motile systems. J Biol Chem 265:8347–8350.

Jaramillo F, Hudspeth AJ (1991) Localization of the hair cell's transduction channels at the hair bundle's top by iontophoretic application of a channel blocker. Neuron 7:409–420.

Jaramillo F, Hudspeth AJ (1993) Displacement-clamp measurement of the forces exerted by gating springs in the hair bundle. Proc Natl Acad Sci USA 90:1330–1334.

Jaramillo F, Howard J, Hudspeth AJ (1990) Calcium ions promote rapid mechanically evoked movements of hair bundles. In: The mechanics and biophysics of hearing (Dallos P, Geisler CD, Matthews JW, Ruggero MA, Steele CR, eds), pp 26–33. Berlin: Springer.

Koyama H, Lewis ER, Leverenz EL, Baird RA (1982) Acute seismic sensitivity in the bullfrog ear. Brain Res 250:168–172.

Kroese ABA, Das A, Hudspeth AJ (1989) Blockage of the transduction channels of hair cells in the bullfrog's sacculus by aminoglycoside antibiotics. Hear Res 37:203–218.

Lewis RS, Hudspeth AJ (1983) Voltage- and ion-dependent conductances in solitary vertebrate hair cells. Nature 304:538–541.

Lombardi V, Piazzesi G, Ferenczi MA, Thirlwell H, Dobbie I, Irving M (1995) Elastic distortion of myosin heads and repriming of the working stroke in muscle. Nature 374:553–555.

Lumpkin EA, Hudspeth AJ (1995) Detection of Ca^{2+} entry through mechanosensitive channels localizes the site of mechanoelectrical transduction in hair cells. Proc Natl Acad Sci USA 92:10297–10301.

Markin VS, Hudspeth AJ (1995) Gating-spring models of mechanoelectrical transduction by hair cells of the internal ear. Annu Rev Biophys Biomol Struct 24:59–83.

Marquis R, Benser ME, Hudspeth AJ (1995) Evoked hair-bundle motility during mechanoelectrical transduction in hair cells of the bullfrog's sacculus. Biophys J 70:A365.

Ogata K (1970) Lead compensation. In: Instrumentation and control series, Prentice-Hall electrical engineering, pp 482–490. Englewood Cliffs: Prentice-Hall.

Okuno M, Hiramoto Y (1979) Direct measurements of the stiffness of echinoderm sperm flagella. J Exp Biol 79:235–243.

Pickles JO, Comis SD, Osborne MP (1984) Cross-links between stereocilia in the guinea pig organ of Corti, and their possible relation to sensory transduction. Hear Res 15:103–112.

Probst R (1990) Otoacoustic emissions: an overview. In: New aspects of cochlear mechanics and inner ear pathophysiology (Pfaltz CR, ed), pp 1–91. Basel: Karger.

Ruggero MA (1992) Responses to sound of the basilar membrane of the mammalian cochlea. Curr Opin Neurobiol 2:449–456.

Russell IJ, Richardson GP, Kössl M (1989) The responses of cochlear hair cells to tonic displacements of the sensory hair bundle. Hear Res 43:55–70.

Russell IJ, Kössl M, Richardson GP (1992) Nonlinear mechanical responses of mouse cochlear hair bundles. Proc R Soc Lond [Biol] 250:217–227.

Shepherd GMG, Corey DP (1994) The extent of adaptation in bullfrog saccular hair cells. J Neurosci 14:6217–6229.

Shotwell SL, Jacobs R, Hudspeth AJ (1981) Directional sensitivity of individual vertebrate hair cells to controlled deflection of their hair bundles. Ann NY Acad Sci 374:1–10.

Thomas RC (1978) Ion-sensitive intracellular microelectrodes. How to make and use them. p 19. London: Academic.

van Netten SM, Khanna SM (1994) Stiffness changes of the cupula associated with the mechanics of hair cells in the fish lateral line. Proc Natl Acad Sci USA 91:1549–1553.

Walker RG, Hudspeth AJ (1996) Calmodulin controls adaptation of mechanoelectrical transduction by hair cells of the bullfrog's sacculus. Proc Natl Acad Sci USA 93:2203–2207.